Choosing Portfolios of Reinforcement Actions for Distribution Grids Based on Partial Information*

Joaquín de la Barra[a,*], Ahti Salo[a] and Mahdi Pourakbari-Kasmaei[b]

[a]Department of Mathematics and Systems Analysis, Aalto University, Finland
[b]Department of Electrical Engineering and Automation, Aalto University, Finland

ARTICLE INFO

Keywords:
Partial information
Decision analysis
Influence diagrams
System reliability
Risk management
Distribution grids

ABSTRACT

The cost-efficiency of individual reinforcement actions in mitigating risks of external hazards in distribution grids depends on the entire portfolio of implemented actions. Thus, when seeking to reinforce distribution grids, it is pertinent to assess *portfolios* of reinforcement actions to account for dependencies between them. Motivated by this recognition, we develop a systemic framework to support Distribution System Operators (DSOs) in allocating scarce resources to portfolios of reinforcement actions that help protect multiple grids against hazards in the light of complementary reliability indices. This decision problem is structured as an influence diagram that contains scenarios representing combinations of realizations for different types of hazards. For cases where scenario probabilities, perceived importance of the grids, and relevance of reliability indices are known, the framework solves a mixed-integer linear programming problem to determine optimal portfolios. If this is not the case, the framework accommodates partial information about these parameters. Building on this partial information, it computes all the non-dominated portfolios by obtaining optimal portfolios for specific parameters and screening the other feasible portfolios. The non-dominated portfolios are analyzed to guide the choice of reinforcement actions at different budget levels. The framework is illustrated with a case study where the DSO seeks to mitigate risks associated with three types of hazards in three distribution grids. The novelty of the proposed optimization-based framework lies in (i) combining Portfolio Decision Analysis (PDA) and reliability models to determine cost-efficient reinforcement portfolios and (ii) accommodating partial information about parameters required by PDA and reliability models.

1. Introduction

As a result of trends such as the electrification of industrial processes, the reconversion of heating systems, and the integration of electromobility, electricity has become the primary energy source in most countries. In this context, the reliability of electricity supply is crucial to ensure the continuity of services offered by critical infrastructures. Because disruptions in electricity supply can cause unacceptable societal impacts, advanced societies expect a highly reliable system. However, achieving a fully reliable system cannot be guaranteed due to the inherent failure rates of technical components and the possibility of excessive loads due to external conditions. There are also intrinsic trade-offs, as introducing more stringent reliability requirements increases the total cost of the power system [1]. Moreover, there is a diminishing marginal utility in safety investments [2]. Consequently, the standard approach is to require that the power system provides energy as economically as possible while meeting the agreed safety and reliability criteria [3].

*This research has been partly supported by Profi-5 project funding granted by the Academy of Finland (funding decision 326346).
*Corresponding author
joaquin.delabarra@aalto.fi (J.d.l. Barra)
ORCID(s): 0000-0003-3878-8289 (J.d.l. Barra); 0000-0003-1526-7923 (.A. Salo); 0000-0003-4803-7753 (.M. Pourakbari-Kasmaei)

Power interruptions can occur due to failures in the generation, transmission, and distribution systems [4]. However, interruptions affecting end consumers are caused primarily by failures at the distribution level [5]. This has driven the development of approaches to reinforce distribution grids to meet specified safety and reliability requirements while minimizing costs. These costs include energy losses, the acquisition of new components, and penalties for violating reliability requirements, which can be monetized and aggregated to facilitate cost-effectiveness analyses. In turn, achieving reliability requirements can be quantified by employing global or local reliability indices. Optimization approaches have been proposed to manage trade-offs between cost and reliability when designing the reinforcement of distribution grids. For example, it is possible to employ single-objective approaches to minimize costs, subject to reliability requirements. Alternatively, one may seek to maximize reliability subject to constraints on the costs of required investments and associated operational expenses. These two objectives can also be pursued jointly. For example, Shang et al. and Zhang et al. propose multi-objective methods to minimize cost and losses while maximizing reliability [6, 7].

Planning reinforcement actions to protect the grids is also challenging due to uncertainties related to different types of hazards, technical faults, and future trends in demand and generation capacity [8, 9]. Thus, to guide investments into reinforcement actions to improve the reliability of distribution grids, one needs first to identify what hazards can affect them. For example, Mahmoud et al. define 14 different categories of hazards that can affect power systems [10]. Hazards that affect grids are usually not mutually exclusive because it is possible that several hazards occur simultaneously or that some hazards may cause others. Accordingly, it is essential to develop scenarios that capture different combinations of hazard realizations instead of treating hazards independently.

From the viewpoint of comprehensiveness, there are benefits to developing the full set of scenarios that represent all relevant uncertainties. This is especially the case in the context of safety-critical systems whose risk analyses are usually required to be conservative (i.e., the results should err on the side of too much caution rather than too little caution [11]). Because hazards may occur jointly, omitting scenarios depicting the joint occurrence of several hazards would violate the principle of comprehensiveness, especially if the resulting loss of reliability is aggravated by such joint occurrence [12]. Šarūnienė et al. propose a methodology based on a Bayesian network and simulation to assess simultaneous risks on interdependent critical infrastructures due to multiple hazards [13]. While this approach successfully identifies critical elements in failure scenarios, it relies heavily on data availability, as estimating conditional probabilities is required in addition to the initial failure probabilities of components. More broadly, the comprehensive modeling of scenarios is often difficult due to the inability to build and access relevant empirical data sets, the lack of time that can be devoted to effective risk communication with decision-makers, or even the challenges of computational complexity [14, 15]. Reasons such as these can make it hard to justify the assignment of exact probabilities to scenarios, particularly those that represent extreme events or pertain to multiple hazard realizations with poorly understood correlations. It is,

therefore, instructive to retain the full set of scenarios, including joint realizations of hazards, while seeking to overcome the difficulties of employing exact probability by admitting partial information about the scenario probabilities.

Once the possible realizations of hazards that may affect distribution grids have been identified, the next step is to assess how these hazards impact system performance. Technically, there are well-established computational models for estimating the reliability of grids in the face of hazards. For example, Ji et al. show that extreme weather exacerbates the vulnerabilities of distribution grids [5]. Hou et al. propose a framework to assess the impact of ice storms on the resilience of distribution systems [16]. Jasiūnas et al. propose a fragility-based power disruption model against windstorms that focuses on the impact on multiple grids in large areas [17]. Atrigna et al. study the effect of heat waves on power distribution grid failures and propose a fault prediction system based on machine learning [18]. Diao et al. evaluate the system failure rates associated with alternative defense strategies against cyber-attacks [19]. The authors acknowledge that it is difficult to predict the likelihood of cyber-attacks, and rather than providing estimations for them, they assume that the attacks are certain events and compute the failure probability of the systems by evaluating the defense actions. Ding et al. present a broad review of cyber-threats and potential responses to them [20]. Bagheri et al., Fan et al. and Pan et al. explore the effects of demand uncertainties and the increasing generation of renewable electricity on the reliability of the distribution grid [21, 22, 23].

In addition to relying on model-based approaches, experts can be consulted to harness a complementary source of information. Expert judgments can be useful both in the early stages of the analysis, when the aim is to characterize possible realizations of hazards, and in the later stages, when the focus is on assessing the impacts of these realizations on critical infrastructures such as distribution grids. In general, expert judgments are particularly relevant in settings where there is a lack of historical data or when the grids must be prepared against hazards that have not occurred, such as intentional attacks [24]. For example, the report [25] illustrates how an extensive range of expert judgments can be generated in developing a national risk assessment study. In the context of power grids, Wu et al. combine Bayesian networks, system dynamics, and the analytic hierarchy process to optimize the investment in safety on the grid [2]. They developed a tool to help decision-makers select power grid safety investments. The five most typical accidents were selected based on the statistical information of the grid to perform the analysis. Choosing accidents based solely on their frequency overlooks low-probability hazards that can significantly impact the grid. Furthermore, this approach fails to account for the potential evolution of hazards that threaten the system since their frequency and severity can increase. The contribution rate of different safety levels is obtained from three safety managers, one safety engineer, and a researcher on safety management. The judgments of these experts are later combined using weights. Combining the expert's judgments makes the optimization problem more tractable and can reduce the number of alternatives; in some cases, however, keeping the judgments separated provides additional information on the system's performance.

Following hazard characterization, the impact of alternative reinforcement actions on the grids' reliability needs to be assessed to build a basis for selecting and implementing actions that mitigate the risks posed by hazards cost-efficiently. Specifically, depending on their technical design and other characteristics, reinforcement actions can be local, in which case they affect just a portion of the grid, or systemic, in which case they affect a more extensive part of the grid or even multiple grids. Capital-intensive measures like infrastructure upgrades are discussed by Amjady et al. and Muñoz-Delgado et al. [26, 27], while operational solutions such as grid reconfiguration are presented by Ahmadi et al. and Azizivahed et al. [28, 29]. Tian et al. enhance the reconfiguration approach by combining it with the pre-allocation of unmanned aerial vehicles to support the restoration of the system [30]. Importantly, the authors acknowledge that these actions are usually planned independently and highlight the benefits of combining them. Sambasivam et al. analyze the effect of the network topology in the optimal placement of generators and storage systems for its restoration after a disaster [31]. Zhao et al. increase the system's resilience against cyber-attacks by strategically allocating energy storage [32]. Hou et al. propose a tri-level optimization framework to increase the resilience of networks against typhoons by hardening the lines, dispatching generation units, and reconfiguring the topology [33]. de la Barra et al. and Franco et al. propose less intensive capital solutions for installing protective devices [34, 35], which has become a timely approach due to the integration of distributed generation [36] and the installation of more sophisticated communication systems [37]. Extensive surveys on ways to improve the reliability of grids, including discussions of relevant objectives and computational algorithms, are presented in [38, 36, 39].

Although each grid can be individually reinforced against specific hazards with the above procedures, there are benefits to reinforcing multiple grids simultaneously by selecting a *portfolio* of several reinforcement actions. By design, choosing such a portfolio is a problem that needs to be approached with Portfolio Decision Analysis (PDA) [40] as the assessment of individual reinforcement actions that focus on one hazard at a time will not reveal how *combinations* of multiple reinforcement actions help mitigate risks posed by several hazards. Against this background, there is a need for systemic approaches that are equipped to accommodate several information sources, such as reliability models and expert consultation, as part of a comprehensive framework that helps assess the cost-efficiency of portfolios of reinforcement actions.

In this paper, we work toward this end by presenting an optimization-based framework to select cost-efficient portfolios of reinforcement actions. This selection problem is structured as an influence diagram, which is then solved with mixed-integer linear programming (MILP) using Decision Programming [41] to identify optimal portfolios of reinforcement actions. The framework accounts for the costs of reinforcement actions and their impacts on the reliability of the grids. Specifically, these impacts depend on the chosen portfolios of reinforcement actions and the scenarios that represent the occurrence of different combinations of hazards. Additionally, the framework admits partial information about the scenario probabilities, multiple information sources, and the DSO's preferences for grids and reliability

indices. The optimal portfolios for different combinations of parameter values are then computed by solving the MILP model. These portfolios are then exploited to identify non-dominated portfolios across the partial information specification. Furthermore, by solving the selection problem at different levels of investment costs, the framework identifies non-dominated portfolios that are cost-efficient in maximizing the reliability of the grids at a given level of total costs, allowing the DSO to make risk-informed decisions about reinforcement actions. The framework is illustrated with a stylized case study[1] in which a DSO evaluates portfolios of reinforcement actions to mitigate the risks posed by three types of hazards in three adjacent distribution grids. We illustrate how differences in the judgments expressed by several experts, illustrated by five vectors of scenario probabilities concerning the occurrence of hazards, can be handled through partial information representing the full range of information sources.

This work contributes to the literature by integrating reliability models for distribution grids and information sources, such as the elicitation of expert judgments, with the use of partial information in PDA to identify cost-efficient risk mitigation portfolios. By incorporating partial information, the proposed framework expands the scope of analysis to situations where decision-makers cannot fully quantify preferences or assign deterministic probabilities to scenarios due to limited information or uncertainty about the future. Moreover, incorporating partial information supplements existing models, enabling their application in contexts where the requisite information for their utilization is not fully available. The framework allows DSOs to adopt a holistic approach to selecting reinforcement actions, addressing multiple hazards while assessing the reliability impacts of portfolios of such actions. Furthermore, by presenting results across different investment levels, the framework illustrates the relationship between investment and reliability, helping DSOs set appropriate investment levels based on the impact of those levels on system reliability.

This paper is structured as follows. Section 2 presents the framework and discusses relationships between reliability models and expert judgments. Section 2.6 formulates the problem of selecting reinforcement actions by presenting the influence diagram and the objective function. Section 3 presents an illustrative case study in which a DSO aims to reinforce three adjacent distribution grids. Section 4 discusses the numerical results, limitations of the framework, and possible extensions. Finally, Section 5 summarizes the contributions of the work and outlines future research areas.

2. Methodology

Our framework helps identify at different investment levels those portfolios of reinforcement actions that are most effective in improving the reliability of multiple interconnected grids. This is achieved by building a structured decision model that accounts for (i) the relevance of reliability indices, (ii) the perceived importance of the grids, and (iii) the probabilities of scenarios representing the occurrence of hazards that impact the grids' reliability. Because complete information about the model parameters may be hard to obtain, the framework admits partial information, which

[1] Possibilities for providing real data on hazards affecting the grids are limited by concerns on confidentiality.

extends its usability to cases where it is not possible or practical to acquire complete information due to resource or time constraints.

In the following, we summarize the main framework assumptions and the employed notation. Then, we describe the required information and the decision model from which the optimal and non-dominated portfolios of reinforcement actions are computed. Because data availability can vary from system to system, we first discuss the characterization of required parameters and partial information. This allows us to provide recommendations for adopting the framework in different contexts.

2.1. Framework assumptions

The main assumptions of the framework are as follows: (i) the portfolio optimization is carried out for the situation where all the selected reinforcement actions will have been implemented (i.e., no intermediate results are provided for the situation where only some of the selected actions have been implemented); (ii) the costs of all reinforcement actions are available before determining which ones will be implemented; (iii) the hazards can be represented by a discrete set of scenarios whose probabilities can be estimated by relying information sources (e.g., simulation, statistical models, expert elicitation, or a combination of these); (iv) failure events are quantified through estimates about failure rates and restoration times; (v) these estimates depend on scenarios and selected reinforcement actions; (vi) the line-specific failure rates can be expressed aggregating the failure rates for different hazards types; (vii) the impacts of failure events can be quantified through reliability indices; (viii) the reliability of one grid does not affect that of others; (ix) reinforcement actions have no impact on scenario probabilities.

2.2. Notation

Table 1 defines the sets in the framework. The decision variables for selecting local and global reinforcement actions are itemized in Table 2. Table 3 lists the reliability parameters for line failure events and parameters that encode the impacts of reinforcement actions and scenarios defined by combinations of alternative realizations of hazards. The parameters that represent scenario probabilities as well as the DSO's preferences for reliability indices and distribution grids are in Table 4. The notation for the influence diagram presented in Section 3.4 and its corresponding MILP formulation is in Table 5.

2.3. Accounting for multiple risk indices and distribution grids

The reliability of distribution grids can be quantified by reliability indices[2] that account for different reliability attributes, such as the frequency or duration of interruptions. The system average interruption duration index (SAIDI) and the system average interruption frequency index (SAIFI) are systemic indices that quantify the average duration

[2] See IEEE guide for electric power distribution reliability indices [42].

Table 1
Definition of sets.

I	Set of hazards types, $I = \{1, ..., n_i\}$
E	Set of information sources (e.g., experts), $E = \{1, ..., n_e\}$
G	Set of grids, $G = \{1, ..., n_g\}$
R	Set of reliability indices, $R = \{1, ..., n_r\}$
H_i	Set of realizations for hazard type $i \in I$
H	Set of scenarios
A	Set of portfolios of local and global reinforcement actions
A_F	Set of feasible portfolios
A_q^g	Set of local reinforcement actions of type $q \in \{1, ..., n_q\}$ for grid $g \in G$
A_k^0	Set of global reinforcement actions of type $k \in \{1, ..., n_k\}$
S_E	Set of scenario probabilities
S_R^g	Set of importance weights for reliability indices in grid $g \in G$
S_G	Set of importance weights for grids
S	Aggregate information set defined by S_E, S_R^g, S_G
$A_N(S)$	Set of non-dominated portfolios for the information set S

Table 2
Definition of decision variables.

a_k^0	Decision variable for selecting a global reinforcement action of type k from $A_k^0, k \in \{1, \dots, n_k\}$
a_q^g	Decision variable for selecting a local reinforcement action of type q for grid g from $A_q^g, g \in G, q \in \{1, \dots, n_q\}$
a	Portfolio of reinforcement actions containing all selected global and local actions, i.e., $a = (a_k^0)_{k=1}^{n_k} \cup (a_q^g)_{g \in G, q=1}^{n_q}$

Table 3
Definition of parameters associated with the reliability of the grids and the impact of reinforcement actions and hazards.

λ_b^l	Basal failure rate of line l [failures/year]
λ_{ib}^l	Basal failure rate of line l for hazard type $i \in I$ [failures/year]
τ_b^l	Basal restoration time of line l [hours/failure]
$f_i^l(h_i)$	Multiplicative factor by which hazard realization $h_i \in H_i$ affects line l failure rate λ_i^l, for hazard type $i \in I$
$t^l(h_i)$	Multiplicative factor by which hazard realization $h_i \in H_i$ affects line l restoration time τ^l, for hazard type $i \in I$
$\iota_i^l(a_q^g)$	Multiplicative factor by which local reinforcement action $a_q^g \in A_q^g$ affects line l failure rate λ_i^l for hazard type $i \in I$
$\iota_i^l(a_k^0)$	Multiplicative factor by which global reinforcement action $a_k^0 \in A_k^0$ affects line l failure rate λ_i^l for hazard type $i \in I$
$\varrho^l(a_q^g)$	Multiplicative factor by which local reinforcement action $a_q^g \in A_q^g$ affects line l restoration time τ^l
$\varrho^l(a_k^0)$	Multiplicative factor by which global reinforcement action $a_k^0 \in A_k^0$ affects line l restoration time τ^l
λ^l	Failure rate of line l [failures/year]
λ_i^l	Failure rate of line l for hazard type $i \in I$ [failures/year]
τ^l	Restoration time of line l [hours/failure]
R_r^g	Normalized value of reliability index $r \in R$ of grid $g \in G$
R^g	Normalized values of all reliability indices $r \in R$ for grid $g \in G$, i.e., $R^g = (R_r^g)_{r \in R}$
U^g	Unreliability of grid $g \in G$
U_{tot}	Aggregate disutility

and frequency of interruptions that affect all grid customers. In contrast, customer interruption duration (CID) and customer interruption frequency (CIF) are local indices for the duration and frequency of interruptions in a particular node. The average system availability index (ASAI) is the ratio of hours that the system was available during a given period. Expected energy not supplied (EENS) estimates the amount of energy the system does not deliver due to failures or insufficient generation capacity. In general, the relevance of these reliability indices depends on the characteristics

Table 4
Definition of parameters associated with scenario probabilities and the DSO's preferences for grids and reliability indices.

h_i	Realization of hazard type $i \in I$
h	Scenario, defined as a combination of one realization per each hazard type, i.e., $h = (h_i)_{i \in I} \in H$
p_h^e	Probability of scenario $h \in H$ as reported by information source $e \in E$
α_e	Importance weight associated with information source $e \in E$
w_g	Importance weight of grid $g \in G$
ω_r^g	Importance weight of reliability index $r \in R$ on grid $g \in G$
p^e	Vector of scenario probabilities based on information source e, i.e., $p^e = (p_h^e)_{h \in H}$
w	DSO's importance weights for grids, i.e., $w = (w_g)_{g \in G}$
ω^g	DSO's importance weights for reliability indices in grid $g \in G$, i.e., $\omega^g = (\omega_r^g)_{r \in R}$

Table 5
Definition of influence diagram notation.

C	Set of chance nodes
D	Set of decision nodes
V	Value node
N	Set of all nodes in the influence diagram, $N = C \cup D \cup V$
S_j	Set of possible states for node $j \in C \cup D$
s	A path $s = (s_j)_{j \in C \cup D}$
$\mathcal{A}$	Set of arcs in the influence diagram, $\mathcal{A} = \{(i,j), i,j \in N\}$
$I(j)$	Information set of node j, $I(j) = \{i \in C \cup D \mid (i,j) \in \mathcal{A}\}$
$s_{I(j)}$	Realization of states of nodes in $I(j)$
$S_{I(j)}$	Set of all possible realizations $s_{I(j)}$
X_j	Random or decision variable associated with node $j \in C \cup D$
$z(s_j)$	Binary variable for decision node $j \in D$, equals 1 if $X_j = s_j$, 0 otherwise
$\mathcal{U}(s)$	Disutility associated with path s
$\pi(s)$	Probability of path s
$p(s)$	Upper bound of path probability, $p(s) = \prod_{j \in C} \mathbb{P}(X_j = s_j \mid X_{I(j)} = s_{I(j)})$

of the grid and even on regulations that may require some specific indices to attain minimum levels. Because several indices can be relevant to the DSO, the priorities ascribed to them represent the specific requirements in a given planning context.

Furthermore, the grids are not all equally important to the DSO and can thus be prioritized depending on the context and the needs of the areas served by the grids. For example, due to their significant social impact, the DSO can focus on protecting critical networks that enable essential services, such as those provided by hospitals. Similarly, it is common practice to prioritize the reliability of residential sectors over industrial ones, especially when industrial customers have backup systems to mitigate potential disruptions.

In summary, the formulation of the decision model may benefit from explicitly incorporating the DSO's preferences regarding (i) the relevance of reliability indices and (ii) the perceived importance of the grids, as these priorities matter in guiding the selection. Such priorities can be elicited, for example, by treating the reliability indices of different grids as multiple criteria so that well-established techniques from multi-criteria decision analysis can be employed to elicit

weight information. An authoritative overview of applicable state-of-the-art elicitation techniques is presented by Dias et al. [24].

2.4. Identification of hazards and quantification of scenario probabilities

Identifying the salient external hazards that can cause disruptions sets the stage for evaluating alternative reinforcement actions. Requisite information about these hazards– stated in terms of (i) the alternative realizations in which the (non)-occurrence of these hazards can manifest and (ii) how probable these realizations are–can be aggregated from many information sources, including systematic reviews of reports on earlier incidents, the development of statistical models, and the consultation of experts. In particular, it is pertinent to consider the possibility that several hazards may occur together. This is because the performance of the grids may then degrade much more than what would be the case if interactions between multiple hazards are not accounted for.

There are numerous techniques for estimating the joint probability distribution of scenarios [43]. For example, one may first elicit marginal probabilities for the possible realizations of individual hazards. If there are dependencies between the hazards, one may elicit first-order or even second-order conditional probabilities to obtain a more accurate description of the joint probability distribution. This description can be based either on point estimates or intervals [44, 45].

In addition, cross-impact analysis methods, such as the approach proposed by Roponen and Salo [46], can be employed to derive scenario probabilities for each expert. For illustrative purposes, we explain how this approach can be implemented once the hazards and their possible realizations have been specified:

1. Experts are presented with historical information on earlier disruptions as well as forecasts concerning relevant variables such as weather conditions or pollution levels. Based on this and other accompanying relevant information, experts are invited to identify relevant hazards and specify viable realizations for them. The resulting characterization needs to be consensual, as it provides the backdrop for the estimation of probabilities.
2. The marginal probabilities for the realizations of each hazard are elicited from every expert. These marginal probabilities convey how likely these realizations are relative to each other when no particular assumptions are made about the occurrence of other hazards.
3. Experts are requested to estimate cross-impacts between realizations for selected hazard pairs. Each cross-impact estimate indicates how much the probability of a given realization of one hazard would change if another hazard has one of its possible realizations.
4. The cross-impact estimates of each expert are transformed into numerical values, known as cross-impact multipliers, which are synthesized to derive the joint probability distribution over all scenarios.

Thus, the above process gives a joint probability distribution over scenarios for each expert. Still, experts may continue to have divergent beliefs about scenario probabilities and need not agree. These divergent beliefs can be captured through partial information, defined as the smallest convex set of probabilities that contains the probabilities provided by the different experts.

2.5. Reliability of distribution grids

The failure events of a line l are traditionally represented by two parameters: the failure rate λ^l [failures/year] and the restoration time τ^l [hours/failure]. These widely used parameters can be estimated from the fault records maintained by the DSO, either to comply with national regulations or for internal risk management purposes. We denote the basal parameters for failure rates and expected restoration time by λ_b^l and τ_b^l, respectively, referring to the numerical values that apply at the outset before the implementation of reinforcement actions and the occurrence of hazards.

Specifically, we quantify the reliability of distribution grids with a model based on [47] that computes the reliability indices SAIDI, SAIFI, MCIF (maximum CIF among the nodes), and MCID (maximum CID among the nodes) from the input parameters λ and τ of each distribution line on the grid, the number of customers per node, and the location of the protective devices. Failures of demand nodes are not considered, but this entails no loss of generality because such failures can be, in principle, represented by introducing additional virtual nodes and lines between them. We do not consider perfectly coordinated reclosers. However, elements of more detailed models can also be included, such as [34, 48] to accommodate different protective devices and coordination requirements between them.

2.5.1. Reliability impact of hazards

The reliability of distribution grids is affected by many types of hazards. Examples include cyber-attacks, major traffic accidents, excessive pollution, or extreme weather conditions. Thus, the first step in risk-informed selection of mitigation actions is to identify what hazards are included in the analysis based on their anticipated impacts and estimated likelihood.

Our framework considers a set of hazards classified into $i \in I = \{1, \dots, n_i\}$ hazard types. A scenario is defined as $h = (h_1, \dots, h_{n_i}), h_i \in H_i, i \in I$ where H_i is the set of alternative realizations (outcomes) for the i-th hazard type. For example, if there are two hazard types cyber-attack (CA) and weather conditions (WC) with two possible realizations for each, we have $H_{CA} = \{CA_0, CA\_\}$ and $H_{WC} = \{WC_0, WC\_\}$ and there are four scenarios (CA_0, WC_0), $(CA_0, WC\_)$, $(CA\_, WC_0)$, and $(CA\_, WC\_)$. In what follows, the realizations with the sub-index "0" represent less harmful realizations associated with the basal reliability parameters.

To account for the impact of the hazards (and later on for reinforcement actions), the basal reliability parameters are modified with multiplicative parameters whose values depend on the occurrence of hazards and implementation of reinforcement actions. For failure rates, we employ the additive model $\lambda_b^l = \sum_{i=1}^{n_i} \lambda_{ib}^l$ where λ_{ib}^l is the basal failure

rate of line l for hazard type i. This extension to multiple failure rates associated with the hazard types requires more analysis, which can limit the number of hazards considered. When there is enough data, it is possible to use statistical models to compute the failures associated with different hazards directly. In other cases, it is possible to estimate them. For example, Wang et al. computes different failure rates for temperature, rainfall, wind, and humidity based on scarce fault records [49].

The impact of the hazard realization h_i on the failure rate λ_i^l is accounted for by the multiplicative factor $f_i^l(h_i)$ so that the resulting failure rate is $\lambda_i^l(h_i) = \lambda_{ib}^l f_i^l(h_i)$. Consequently, $\lambda^l(h) = \sum_{i=1}^{n_i} \lambda_i^l(h_i)$ is the failure rate of the line l in scenario h. These multiplicative factors are indexed by l because hazards may not affect all lines. If the hazard does not impact the line, the multiplicative factor is 1.

The expected restoration time τ [hours/failure] does not depend on the type of hazard that causes the failure. This means that we assume that if a hazard affects the restoration time, it will affect it for any disruption. For example, adverse weather conditions can delay maintenance crews, increasing the restoration time of disruptions caused by other hazards. Still, the reliability indices that quantify the duration of failures (SAIDI and CID) depend on the hazard types because the duration is also affected by the number of failures. The framework can be readily extended to include restoration times depending on hazard types by using the same structure used for failure rates.

The multiplicative factors can be obtained by applying statistical analysis to the historical data. The primary source of this data is the DSOs, who are obliged by law to register the failure events affecting the distribution grids [50]. The statistical analysis depends on the data availability and the nature of the hazards affecting the system. We provide some instructive examples for analyzing the failure events on distribution systems to quantify failures for different hazards. Clavijo-Blanco and Rosendo-Macías create a methodology to estimate failure rates for different hazards [50]. Alvehag and Soder present a model in which the failure rate of an over headline is the sum of the failure rate during normal weather conditions and the failure rate during high winds [51]. Zhou et al. propose a Bayesian Network, which uses conditional probabilities of failures given different weather states [52]. Macedo et al. propose a methodology to assess the reliability of transmission lines for uncertain wind speed and tornado trajectories [53]. Liang and Xie quantify the probabilities of correlated failures of components in a substation during a seismic event [54]. Shafieezadeh et al. propose a framework for developing age-dependent fragility curves of utility wood poles exposed to harsh wind conditions [55]. Ghasemi et al. present an overview of modeling methods to estimate failure rates, including models that study explanatory variables such as environmental conditions [56].

2.5.2. Reliability impact of reinforcement actions

Reinforcement actions modify failure rates and restoration times or install protective devices, which are included directly in the reliability model [47]. We consider a multiplicative model for the case in which the reinforcement

actions modify the failure rates or the restoration times. These actions modify specific failure rates λ_i^l, associated with the i-th hazard type. For example, the underground of a line reduces the failure rates associated with extreme weather conditions, but it does not modify the failure rates associated with cyber-attacks. The impact of the reinforcement actions on specific failure rates is modeled by categorizing the reinforcement actions into different types and estimating corresponding multiplicative factors depending on the hazard type and action type.

We distinguish between global actions, which affect all the grids, and local actions, which affect a single grid. A_q^g denotes the set of local actions of type $q = 1, \dots, n_q$ on grid $g = 1, \dots, n_g$. Similarly, A_k^0 is the set of global actions of type $k = 1, \dots, n_k$. The set of all portfolios, defined as all combinations of local and global actions, is $A = \prod_{g=1}^{n_g} \prod_{q=1}^{n_q} A_q^g \prod_{k=1}^{n_k} A_k^0$. A local action is denoted by $a_q^g \in A_q^g$, a global action by $a_k^0 \in A_k^0$, and a portfolio by $a \in A$. Typically, resource constraints and logical dependencies between reinforcement actions reduce the number of feasible portfolios. For example, a local action may only be viable if a specific global action is implemented. Actions may be mutually exclusive due to resource constraints, for example, when there is not enough personnel to implement them. Lastly, the total investment budget may restrict what actions can be implemented. The set of feasible portfolios $A_F \subseteq A$ consists of those combinations of actions that satisfy all relevant constraints.

The failure rate of a line l in the grid g, considering the combined effects of hazards and reinforcement actions, is calculated using (1). In this equation, $\iota_i^l(a_q^g)$ and $\iota_i^l(a_k^0)$ are the multiplicative factors of the q-th local action type and k-th global action type in the failure rate associated with the i-th hazard type. If an action does not impact the failure rate, this factor equals one.

$$\lambda^l(h, a) = \sum_{i=1}^{n_i} \lambda_i^l(h_i, a) = \sum_{i=1}^{n_i} \lambda_{ib}^l f_i^l(h_i) \prod_{k=1}^{n_k} \iota_i^l(a_k^0) \prod_{q=1}^{n_q} \iota_i^l(a_q^g). \tag{1}$$

The expected restoration time is given by (2), with $t^l(h_i)$, $\varrho^l(a_q^g)$, and $\varrho^l(a_k^0)$ the multiplicative factors of the i-th hazard type, q-th local action type and k-th global action type on the restoration time of line l. If the hazard type i does not impact the restoration time of the line, $t^l(h_i)$ is equal to one. Similarly, if an action does not impact the restoration time, the associated factor equals one.

$$\tau^l(h, a) = \tau_b^l \prod_{i=1}^{n_i} t^l(h_i) \prod_{k=1}^{n_k} \varrho^l(a_k^0) \prod_{q=1}^{n_q} \varrho^l(a_q^g). \tag{2}$$

Estimating multiplicative factors for the impact of reinforcement actions on failure rates or restoration times is difficult due to the paucity of relevant data. Recognizing these challenges, we provide some references that can guide the estimation of multiplicative factors for further studies. One common practice is to compare data from similar systems to isolate the effect of the reinforcement action. For example, Fenrick and Getachew estimate the reliability

impact of underground lines based on data from 163 distribution utilities in the US [57]. Although this procedure helps quantify the reliability impact, it cannot be taken for granted that this impact will be the same on a different system. Hughes et al. propose a hybrid physical and data-driven model to assess the impacts of pole replacement, pole class upgrade, improved pole chemical treatment, and undergrounding to reduce pole failures [58]. Taylor et al. propose a machine learning outage prediction model to assess the impact of vegetation management on outages in the distribution grid during storm events [59]. Hughes et al. propose a hybrid mechanistic-data-driven outage prediction model to assess the impact of tree trimming and pole replacements in reducing the failures in the grid [60].

2.6. Problem representation

2.6.1. Influence diagram

Influence diagrams give a visual representation of uncertainties (e.g., chance node for scenarios representing hazards), decisions (e.g., decision nodes for reinforcement actions), and consequences (e.g., value node for the reliability of the grids), which helps communicate the structure of multi-stage decision problems under uncertainty. Therefore, they have been used in practical applications to support decision makers (see e.g., [61, 62]).

The influence diagram for the problem of reinforcing n_g grids is shown in Figure 1. The arcs between the nodes denote dependencies: the realization of uncertain events at a chance node is conditionally dependent on its parent nodes from which there is an incoming arc to the chance node. Similarly, arcs pointing to a decision node indicate what information is available at the decision node, while the consequences at the value node are determined by a function whose arguments consist of the states of its parent connected nodes.

The chance node W represents the occurrence of hazards. Its states are scenarios $h \in H$ that represent combinations of realizations of hazard types. Decision node D_G represents the selection of global reinforcement actions, and its states represent portfolios of such actions. Decision nodes $D_g, g \in \{1, ..., n_g\}$ represent the selection of local reinforcement actions for each grid g, where each state corresponds to a specific portfolio of actions for that grid. When reinforcement actions are selected, it is unknown which hazards will occur, if any. This is conveyed by the absence of arcs from node W to decision nodes D_G and $D_g, g \in \{1, ..., n_g\}$. Instead, the actions fortify the grids by improving their reliability to an extent that depends on what other actions are implemented and what hazards occur. Although the decision nodes are presented separately for clarity, these decisions are made simultaneously in a coordinated manner. This coordination accounts for interdependencies, such as those arising from budgetary constraints or logical relationships between decisions.

Chance node G_g represents the realized reliability of the grid $g \in \{1, ..., n_g\}$. This reliability depends on (i) the occurrence of hazards, represented by the scenario (state at W) and (ii) the selection of global and local reinforcement actions at nodes D_G and D_g, respectively. In Figure 1, these dependencies are shown in red and blue. The probability

distribution at node G_g depends on the chosen reliability model to compute its reliability indices. We employ a deterministic model that attaches a unique value to each reliability index for a given scenario and a portfolio of reinforcement actions. This facilitates the interpretation of the ensuing numerical results as uncertainties pertain to scenarios and their probabilities only. Yet, other models, such as [63, 64], can also be employed to accommodate probability distributions for the reliability indices without altering the framework's structure or computational performance. The states of the nodes G_g are defined by discretizing the range of reliability index values across all reinforcement actions and scenarios into five equal-length intervals. This discretization provides a representation of continuous indices and can be refined by increasing the number of states to achieve higher granularity.

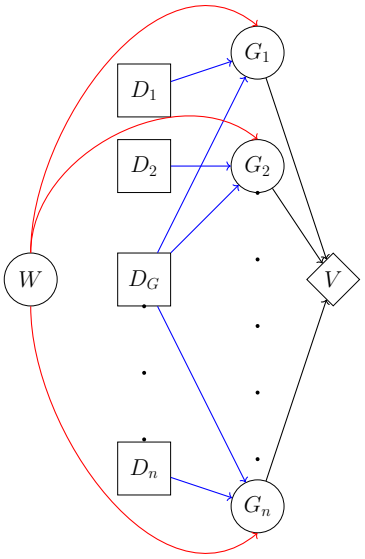

Figure 1: Influence diagram for selecting portfolios of reinforcement actions in the face of external hazards. Chance nodes (circles) represent uncertain events. Decision nodes (squares) represent selections of reinforcement actions. The value node (diamond) represents the consequences of the reinforcement decisions and the realization of uncertainties at the chance nodes.

2.6.2. Unreliability and disutility functions

We frame the portfolio selection problem as minimizing the unreliability of the grids. This is consistent with the interpretation of reliability indices for which higher values represent a less reliable system. For each reliability index $r \in R$ and grid $g \in G$, the indices are represented with a real-valued index function $R_r^g : \mathbb{R} \to [0, 1]$ that maps the values of the reliability index of the grid onto the interval $[0, 1]$. The vector $R^g(h, a) = (R_1^g(h, a), \ldots, R_{n_r}^g(h, a))$ contains these evaluations based on the reliability indices $r \in \{1, \ldots, n_r\}$ for a given scenario h and a portfolio of actions a.

In [65], reliability indices are combined into a single value representing the grid's unreliability. We follow a similar approach, combining the index functions R_r^g into a grid unreliability function

$$U^g(\omega^g, h, a) = \sum_{r=1}^{n_r} \omega_r^g R_r^g(h, a), \tag{3}$$

where the DSO's priorities concerning the significance of reliability indices (see Section 2.3) are represented by the weights ω_r^g. The vector $\omega^g = (\omega_1^g, \ldots, \omega_{n_r}^g)$ contains the weights for each index r reliability index of grid g. These weights can vary for different grids to address specific planning requirements. For example, the SAIDI is more critical than the SAIFI if a grid has backup systems, such as batteries. The weights for the reliability indices are contained in a matrix of dimensions $n_g \times n_r$, i.e., $\omega = (\omega^1; \ldots; \omega^{n_g})$.

Finally, the reliability indices for the grids are combined in an aggregate disutility function

$$U_{tot}(w, \omega, h, a) = \sum_{g=1}^{n_g} w_g U^g(\omega^g, h, a), \tag{4}$$

which reflects the DSO's priorities regarding the different grids and their unreliability. This function takes values from 0 to 1 so that 1 represents the maximum unreliability the hazards may cause if no reinforcement actions are implemented. This additive function U_{tot} allows different priorities to be assigned to the grids. For example, more weight can be given to grids whose reliability is of particular importance because they secure the electricity supply to critical infrastructures.

Combining all of the above, the expected disutility for the portfolio of reinforcement actions a and scenarios $h \in H$ is

$$\mathbb{E}[U_{tot}(p^e, w, \omega, h, a)] = \mathbb{E}[U_{tot}] = \sum_{h=1}^{n_h} p_h^e U_{tot}(w, \omega, h, a), \tag{5}$$

where p_h^e is the probability of scenario h in the vector of scenario probabilities p^e obtained from the source e. This source can be, for example, an expert who provides estimations about the scenario probability. Because the expectation (5) depends on the scenario probabilities $p^e = (p_1^e, \ldots, p_{n_h}^e)$, the expected disutilities of reinforcement portfolios typically vary from one expert to the next. This implies that optimal portfolios can also vary.

2.7. Inclusion of partial information

In this framework, portfolios of reinforcement actions that minimize expected disutility in (5) can be computed by using Decision Programming [41] to solve the mixed-integer linear programming problem for the influence diagram in Figure 1. The key parameters in this problem are (i) the basal reliability parameters of the grids, (ii) the multiplicative

factors for the impact of the actions in scenarios, (iii) scenario probabilities, and (iv) priority weights for the reliability indices and the grids.

However, information about these parameters may be uncertain. The basal reliability parameters may not be valid if they have been derived from scarce data or if reference values have been taken from a different system. The same uncertainty affects the accuracy of the multiplicative factors in the impact assessment of hazards and reinforcement actions. Moreover, the DSO may need to consider a range of priorities for the grids, depending on foreseen demands and even the regulatory context. Also, if additional reliability indices are incorporated, their relevance relative to the ones employed previously needs to be re-evaluated, which may motivate changes in the respective weights. Similarly, connecting new demand points with specific reliability requirements may imply that the DSO needs to ascribe higher priority weights to some indices. Lastly, when multiple experts are consulted to obtain estimates about the scenario probabilities, retaining the full diversity of these probabilities in the analysis may be instructive instead of synthesizing a single vector of scenario probabilities from them. The same situation may apply when considering priority weights for reliability indices and grids because, within the DSO, there may be different viewpoints on what weights are adequate.

Thus, instead of presuming that complete information about the above model parameters can be specified, we consider what decision recommendations can be offered when these parameters are not specified as point estimates but can assume any values within their *feasible information sets*. Thus, these information sets represent *partial information* that can be synthesized with Portfolio Decision Analysis [66, 40] to support decisions in the presence of partial information. In particular, we accommodate partial information about the scenario probabilities and the weights representing priorities for grids and reliability indices. The extension to admit partial information about the basal reliability parameters and the multiplicative factors employed in impact assessment can be pursued analogously.

Because the probabilities of the n_h scenarios add up to one, the set of all possible scenario probabilities S_E^0 is the absence of any constraining information is

$$p \in S_E^0 = \left\{ p \in \mathbb{R}^{n_h} \mid p_h \geq 0, \sum_{h=1}^{n_h} p_h = 1 \right\},$$

where p_h is the probability of the scenario h in the vector of scenario probabilities $p = (p_1, ..., p_{n_h})$. We model partial information about scenario probabilities by assuming that these probabilities belong to the set $S_E \subseteq S_E^0$. Thus, at one extreme, if there is no information about the scenario probabilities, this set contains all the probability vectors in S_E^0. At the other extreme, the case of *complete information* would be represented by the situation where S_E contains only a single vector from S_E^0.

To illustrate the modeling of partial information that draws on multiple sources of expertise $e \in E$, consider a situation in which there are n_e experts such that each expert e provides a point estimate $p^e \in S_E^0$ for the scenario

probabilities. In this case, the relevant set of scenario probabilities can be represented by the feasible information set $S_E \subset S_E^0$

$$p \in S_E = \left\{ \sum_{e=1}^{n_e} \alpha_e p^e \in \mathbb{R}^{n_h} \mid \alpha_e \geq 0, \sum_{e=1}^{n_e} \alpha_e = 1 \right\}, \tag{6}$$

which contains the estimates provided by all experts as well as all convex combinations of such estimates, obtained as weighted averages of these estimates.

In the same way, partial information about the DSO's priorities for the reliability indices, reflected by the weights $\omega^g = (\omega_1^g, \ldots, \omega_{n_r}^g)$, can be specified by choosing a relevant subset S_R^g from the set S_R^0 defined by (7). The absence of any information about priorities for reliability indices would correspond to $S_R^g = S_R^0$. Conversely, if S_R^g contains only a single weight vector, then there is complete information about the priorities. Finally, priorities concerning the grids, represented by the weights $w = \{w_1, \ldots, w_{n_g}\}$, can be modeled as in the case of reliability indices so that these weights are constrained to belong to the set (8).

$$S_R^0 = \left\{ \omega^g \in \mathbb{R}^{n_r} \mid \omega_r^g \geq 0, \sum_{r=1}^{n_r} \omega_r^g = 1 \right\} \tag{7}$$

$$S_G^0 = \left\{ w \in \mathbb{R}^{n_g} \mid w_g \geq 0, \sum_{g=1}^{n_g} w_g = 1 \right\} \tag{8}$$

To explore the full implications of these three sets of partial information, we define the aggregate information set $S \equiv S_E \times S_G \times S_R$ as their Cartesian product. A singleton element of this set $(p, w, \omega) \in S$ thus corresponds to a situation with complete information about the parameters, i.e., the probabilities of the scenarios as well as the weights that are employed to represent priorities for the grids and the reliability indices. For such specification of model parameters, a well-defined optimal portfolio of reinforcement actions would exist that minimize the aggregate disutility function in (5). Yet, given the specification of partial information, there is a need for analytical concepts that permit such information to be processed into defensible decision recommendations as to which portfolios of reinforcement actions outperform others in view of all this information. Towards this end, we introduce the following dominance relation between pairs of feasible portfolios of reinforcement actions $a, a' \in A_F$ as follows;

Definition 1. *Let $a, a' \in A_F$. Then portfolio a dominates a' with regard to the information set S, denoted by $a \succ_s a'$, if and only if $\mathbb{E}[U_{tot}(p, w, \omega, h, a)] \leq \mathbb{E}[U_{tot}(p, w, \omega, h, a')] \forall (p, w, \omega) \in S$ and the inequality is strict for some $(p, w, \omega) \in S$.*

Specifically, if the portfolio a' is dominated by portfolio a, the expected aggregate disutility reduction in (5) for a' cannot be greater than that for a. Moreover, for some parameters, (p, w, ω) in the information set S, portfolio a gives a greater reduction in disutility. Thus, a DSO that seeks to minimize the expected disutility should not choose dominated portfolios and can focus its attention on non-dominated portfolios. Although Definition 2 is in terms of expected disutility, other metrics such as Conditional Value at Risk (CVaR) can be considered, particularly for focusing on extreme adverse outcomes (see, e.g., [67]). The non-dominated portfolios depend on the information set S and the constraints determining what portfolios are feasible.

Definition 2. *A feasible portfolio $a \in A_F$ is non-dominated for the information set S if and only if there is no feasible portfolio $a' \in A_F$ such that $a' \succ_s a$.*

The set of non-dominated portfolios for the information set S, denoted by $A_N(S)$, is computed by first identifying the portfolios that minimize the expected aggregate disutility at the extreme points of S. These portfolios are, by construction, non-dominated. Next, other feasible portfolios are compared against this initial set to assess whether they are non-dominated. If this is the case, they are added to $A_N(S)$; otherwise, they are excluded from consideration. Algorithm 2 in Appendix A gives a step-by-step description of this approach, which is computationally efficient because portfolios of reinforcement action can be compared based on their aggregate expected disutility at the extreme points of the information set.

Because the non-dominated portfolios contain different actions $a \in A_N(s)$, further solution concepts are needed to generate recommendations for making choices between actions. For this purpose, the *core index* of Robust Portfolio Modeling [66, 68] is useful as it indicates the share of all non-dominated portfolios in which a given reinforcement action is contained.

Definition 3. *The core index of the global reinforcement action $a_k^0 \in A_k$ for the information set S is*

$$CI(a_k^0, S) = \frac{|\{a \in A_N(S) \mid a_k^0 \in a\}|}{|A_N(S)|}$$

and similarly, for the local action $a_q^g \in A_q$ in grid g, the core index is given by

$$CI(a_q^g, S) = \frac{|\{a \in A_N(S) \mid a_q^g \in a\}|}{|A_N(S)|}$$

where $|\{\cdot\}|$ denotes the number of portfolios in the set.

If the core index of a reinforcement action is 1, this action is in all non-dominated portfolios and should be selected in light of the parameters in the information set. Conversely, if the core index of an action is 0, this action is not

in any non-dominated portfolio. It can thus be rejected because selecting such an action would inevitably lead to a dominated portfolio. If the specification of the partial information becomes more conclusive in the sense that the updated information set becomes a proper subset of the initial one, some previously non-dominated portfolios may become dominated, but no new non-dominated portfolios will be found. This implies that if gradual information refinement converges to a singleton point in the interior of the initial information set, any action with core index 1 will be contained in the optimal portfolio for this singleton point.

3. Case study

We present an illustrative case study in which a DSO is about to invest in a portfolio of reinforcement actions to mitigate the risks arising from three types of hazards (i.e., adverse weather conditions, cyber-attacks, and grid overloading) that affect three adjacent distribution grids. As access to real-world grid information and failure events is limited due to security and privacy concerns, for example, because sharing detailed grid topologies can increase vulnerability to cyber-attacks or physical threats, we adopt the topologies of well-established synthetic networks: the IEEE 33-bus system (Grids 1 and 2) and the IEEE 69-bus system (Grid 3), representing radial distribution systems. Baseline reliability parameters before reinforcement on the number of customers and detailed network topologies are from [69].

The DSO seeks to choose a portfolio of reinforcement actions that maximizes the reliability of grids in view of the four reliability indices that quantify the frequency and duration of disruptions. We consider complete and partial information about the scenario probabilities as well as the DSO's preferences for reliability indices and grids. For complete information, in which case there are exact point estimates for all model parameters, the optimal portfolios are determined by using Decision Programming to formulate a MILP model that corresponds to the influence diagram [41]. For partial information, in which case parameter values are characterized by feasible information sets, we employ Algorithm 2 (see Appendix A) to determine all non-dominated portfolios and analyze these to derive the corresponding core index values for global and local reinforcement actions. These core index values are then examined to generate decision recommendations.

3.1. DSO's priorities for reliability indices and grids

The relevance of reliability indices may depend on the grid characteristics and regulations. We assume that the DSO has four distinct estimates concerning the relevance of the reliability indices, which are referred to as cases. In **Case 1** and **Case 2**, all attention is paid to a single reliability index, considering only SAIDI and SAIFI, respectively. In **Case 3**, SAIDI and SAIFI are equally important. In **Case 4**, the four indices are considered simultaneously; the most

weight is given to the systemic indices SAIDI and SAIFI, while two local indices MCIF and MCID have less weight. The weights ω for these four cases are in Table 6.

Table 6
Weights for reliability indices weights in the four cases.

Cases	$\omega = (\omega_{SAIDI}, \omega_{SAIFI}, \omega_{MCIF}, \omega_{MCID})$
Case 1	(1, 0, 0, 0)
Case 2	(0, 1, 0, 0)
Case 3	(0.5, 0.5, 0, 0)
Case 4	(0.4, 0.4, 0.1, 0.1)

If there is no information on the importance of the four reliability indices, the weight set for these indices is $\omega \in S_R^0 = \{\omega \in \mathbb{R}^4 \mid \omega_r \geq 0, \sum_{r=1}^{n_r=4} \omega_r = 1\}$. To consider the four cases in Table 6, we use the information set $\omega \in S_R = \{\sum_{c=1}^{4} \beta_c \omega^c \in \mathbb{R}^4 \mid \beta_c \geq 0, \sum_{c=1}^{4} \beta_c = 1\} \subset S_R^0$, which contains the weights $\omega^c, c = 1, \ldots, 4$ for the four cases and all the convex combination thereof. Note that because Case 3 is a convex combination of Cases 1 and 2, it need not be explicitly retained to produce numerical results.

Analogously, the DSO's priorities for the three grids are given by the weights $w = (w_1, w_2, w_3)$ where w_g is the weight of grid g. We first consider a situation in which there are no restrictions on these weights, reflecting the assumption that the DSO is either reluctant or unable to specify priorities for the grids. The set of feasible grid weights is $S_G^0 = \{w \in \mathbb{R}^3 \mid w_g \geq 0, \sum_{g=1}^{n_g=3} w_g = 1\}$.

In this situation, non-dominated portfolios are combinations of reinforcement actions that improve the reliability of at least one grid significantly without necessarily improving the reliabilities of the other grids. Thus, it represents a conservative approach in seeking to achieve a balance between the three grids. At the other end of the spectrum, we consider equal weights such that $w_1 = w_2 = w_3 = \frac{1}{3}$ or, in vector notation, $w = \left(\frac{1}{3}, \frac{1}{3}, \frac{1}{3}\right) \in S_G^0$.

3.2. Hazards and scenarios

We consider three types of hazards, denoted by i: (i) adverse weather conditions, (ii) cyber-attacks, and (iii) overloading due to unexpected operational conditions. Each hazard type i can realize in one of several states h_i: for weather conditions, $h_i \in \{WC_0, WC_-, WC_=\}$; for cyber-attacks, $h_i \in \{CA_0, CA_-\}$; and for overloading, $h_i \in \{OL_0, OL_-\}$. The impacts caused by the hazards realizations are quantified by the triplets (affected lines, f_i^l, t^l) in Table 7, whose numerical values are illustrative yet aligned with some earlier studies (e.g., [52, 53]). In general, realistic values can be generated using the references in Section 2.5.1. The "affected lines" indicator in the triplet indicates how many lines in the entire distribution grid are affected by hazards. For example, some lines may be more exposed to weather events than others. The symbol ∀ indicates that all lines are affected. A line that is not affected by a hazard has the corresponding multiplicative factor 1.

Weather conditions affect the failure rate parameter λ and the restoration time τ for each line.[3] For example, the weather conditions $WC_{\_}$ are represented by the triplet (∀, 1.4, 1.4), which means that the failure rates and the expected repair times of all lines will increase by a factor of 1.4. This can be contrasted with $WC_{=}$, which represents more severe weather conditions in which the failure rates and expected repair times of all lines increase by a factor of 2. Cyber-attacks primarily affect the failure rate of specific lines, targeting the most vulnerable and critical ones. To quantify this, we rank the lines based on the product of their failure rate and the number of downstream customers (i.e., the number of customers without supply if the line is disrupted). For instance, a cyber-attack CA, represented by the triplet (4, 3.0, 1.0), increases the failure rate of the four most critical lines by a factor of 3, based on this ranking. The impacts of overloads can be evaluated using power flow models to assess the consequences of increased demand. However, for consistency and comparability, we aggregate these consequences using the same technique as in the case of cyber-attacks, but with different criteria. The lines subject to overload are selected based solely on the number of customers they supply. Note that the ranking criteria used for cyber-attacks and overloading are illustrative and not restrictive. The framework allows flexibility, enabling the specification of affected lines directly instead of using rankings. One could also define another ranking system.

Table 7
Possible hazards and illustrative factors representing their impacts on the grids.

Hazard realization (h_i)	Hazard type (i)	(affected lines, f_i^l, t^l)
$WC_{\_}$	Weather conditions	(∀, 1.4, 1.4)
$WC_{=}$	Weather conditions	(∀, 2.0, 2.0)
CA	Cyber-attacks	(4, 3.0, 1.0)
OL	Overloading	(4, 2.0, 1.0)

Because there is a distinct scenario for every combination of realizations for the three types of hazards (three alternative realizations of weather conditions plus two representing the (non)occurrence of cyber-attacks and overload), the total number of scenarios is $n_h = 12$. For illustration purposes, a hypothetical situation is considered, where estimates of the probabilities of these scenarios are elicited from $n_e = 5$ experts who first assess the marginal probabilities for extreme weather conditions, followed by the assessment of conditional probabilities for cyber-attacks, and finally, conditional probabilities for overloads. Section 2.4 describes one possible procedure for obtaining these values, but other methodologies can also be employed.

For example, the probabilities of Expert 1 are in Table 8, proceeding from the elicitation of marginal probabilities for the weather conditions to the elicitation of conditional probabilities for cyber-attacks and, finally, overloading. The scenario probabilities in Table 9 for the five experts can be readily inferred from this table. For example, the probability of scenario $h_0 = (WC_0, CA_0, OL_0)$ for Expert 1 is $p^1(h_0) = \mathbb{P}[WC_0] \times \mathbb{P}[CA_0 \mid WC_0] \times \mathbb{P}[OL_0 \mid (WC_0 \cap CA_0)] =$

[3] We do not address differences in how the geographical variability in the weather patterns would affect the restoration time for different lines.

Table 8
Vector of scenario probabilities for Expert 1.

Hazards	**Realizations**											
Weather Conditions	WC_0 60%				WC_- 30%				$WC_=$ 10%			
Cyber-attacks	CA_0 50%		CA_- 50%		CA_0 30%		CA_- 70%		CA_0 10%		CA_- 90%	
Overloading	OL_0 80%	OL_- 20%	OL_0 70%	OL_- 30%	OL_0 50%	OL_- 50%	OL_0 40%	OL_- 60%	OL_0 20%	OL_- 80%	OL_0 10%	OL_- 90%
Scenario probabilities	24%	6%	21%	9%	5%	5%	8%	13%	0%	1%	1%	8%

$0.6\times0.5\times0.8 = 24\%$. The information set of scenario probabilities consists of the convex combinations of the experts' estimates $p \in S_E = \{\sum_{e=1}^{n_e=5} \alpha_e p^e \in \mathbb{R}^{12} \mid \alpha_e \geq 0,\ \sum_{e=1}^{n_e=5} \alpha_e = 1\}$.

Table 9
Scenario probabilities by expert.

Scenario	Expert 1	Expert 2	Expert 3	Expert 4	Expert 5
(WC_0, CA_0, OL_0)	24%	26%	16%	10%	5%
(WC_0, CA_0, OL_-)	6%	6%	4%	10%	5%
(WC_0, CA_-, OL_0)	21%	6%	14%	8%	4%
(WC_0, CA_-, OL_-)	9%	2%	6%	12%	6%
(WC_-, CA_0, OL_0)	5%	14%	6%	4%	3%
(WC_-, CA_0, OL_-)	5%	14%	6%	8%	6%
(WC_-, CA_-, OL_0)	8%	5%	11%	6%	4%
(WC_-, CA_-, OL_-)	13%	7%	17%	22%	17%
$(WC_=, CA_0, OL_0)$	0%	2%	0%	0%	1%
$(WC_=, CA_0, OL_-)$	1%	8%	2%	2%	4%
$(WC_=, CA_-, OL_0)$	1%	1%	2%	2%	5%
$(WC_=, CA_-, OL_-)$	8%	9%	16%	16%	41%

3.3. Reinforcement actions

The six types of reinforcement actions in Tables 10 and 11 have either a global impact, affecting the reliability of the three grids, or a local impact, limited to a single grid. The second column indicates for which hazard the failure rate is reduced. For example, reinforcing the communication system reduces the failure rates for cyber-attacks but not for overloading. Some reinforcement actions, such as dispatching maintenance crews or introducing protective devices, are not linked to hazards because they have no direct impact on failure rates.

Specifically, the impacts for reinforcement action are modeled using triplets of illustrative parameter values (affected lines, ι_i^l, ϱ^l). As in the case of modeling hazards, the "affected lines" specify how many lines are impacted by the action. For example, if the selected reinforcement action is UL_+, the most critical line based on failure rates and the number of customers served will be underground. If the decision is to implement the reinforcement action UL_{++}, then the two most critical lines are underground. In practice, these values can be quantified by employing reliability

models or eliciting expert judgments (see 2.5.2 for some references). The impacts are deterministic in that the factors in Tables 10 and 11 quantify the impact of the actions unequivocally.

Table 10
Global actions. ST: Spare Transformer, MC: Maintenance Crew.

Action (a_k^0)	Type (k)	Hazard type (i)	(affected lines, ι_i^l, ϱ^l)	Cost
ST_+	ST	Overloading/Weather	(1, 0.5, 1.0)	200
MC_+	MC	-	($\forall$, 1.0, 0.8)	200

Table 11
Local actions. PR: Protective devices, UL: Underground line, CS: Communication system update.

Action (a_q^g)	Type (q)	Hazard type (i)	(affected lines, ι_i^l, ϱ^l)	Cost
PR_+	PR	-	(3, 1.0, 1.0)	20
PR_{++}	PR	-	(9, 1.0, 1.0)	120
UL_+	UL	Weather	(1, 0.0, 1.0)	50
UL_{++}	UL	Weather	(2, 0.0, 1.0)	100
CS_+	CS	Cyber-attacks	(1, 0.5, 1.0)	30
CS_{++}	CS	Cyber-attacks	(5, 0.5, 1.0)	150

The set of feasible portfolios consists of all possible combinations of reinforcement actions that satisfy the following constraints: (i) only one action for a given reinforcement type can be implemented in each grid, and (ii) the total cost of the reinforcement actions does not exceed the budget representing the investment level (this level can be varied to explore the impacts of the budget on the recommended portfolios). There are two implementation options for the two global reinforcement actions on spare transformers and maintenance crews, and consequently, there are $2^2 = 4$ alternative global reinforcement decisions. There are three types of actions for local reinforcement actions with three implementation options for each action, so each grid has $3^3 = 27$ decision alternatives. This leads to a total of $4 * 27^3 = 78,732$ portfolios.

The cost of a portfolio[4] is the sum of the reinforcement actions contained in it. Thus, we do not account for possible cost synergies (i.e., the aggregate cost associated with implementing two or more actions jointly is the same as what would be the case if these actions were to be implemented separately). However, such cost synergies can be incorporated into the optimization model by introducing dummy variables because they only affect the cost feasibility of the portfolios.

3.4. Influence diagram and MILP formulation

Figure 2 presents the influence diagram. For the case of complete information of model parameters, the solution of this diagram gives the optimal portfolio of reinforcement actions that minimizes the disutility at the value node.

[4]This cost data is system-dependent as the costs for different grids can be very different. Thus, these numerical cost parameters are illustrative and should be considered as examples rather than as precise values that could be applied to all systems.

To obtain this solution, we use Decision Programming [70] to formulate the corresponding MILP model. In the following, we summarize the influence diagram and present an overview of this MILP. For details on converting influence diagrams into MILP models, see [41] and [70].

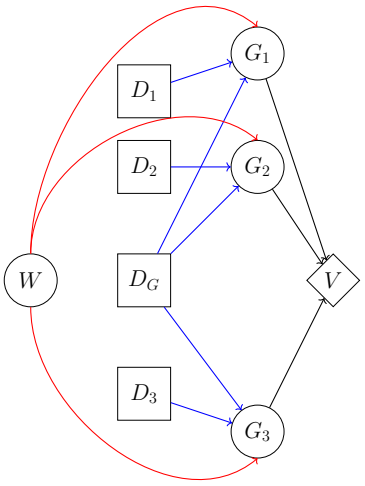

Figure 2: Influence diagram for selecting reinforcement action portfolios to protect three distribution grids from external hazards.

Let $C = \{W, G_1, G_2, G_3\}$ and $D = \{D_G, D_1, D_2, D_3\}$ denote the sets of chance and decision nodes, respectively, and V be the value node in the influence diagram, with $N = C \cup D \cup V$. Every node $j \in C \cup D$ has a finite set of states S_j. At the decision node D_G, the state s_j corresponds to a decision about global reinforcement actions. Analogously, the states at decision nodes D_1, D_2, and D_3 correspond to the decisions about respective local reinforcement actions. Portfolios of reinforcement actions consist of combinations of decisions that are taken across all decision nodes. The states of the chance node W correspond to the 12 scenarios in Table 9. The states of chance nodes G_1, G_2, and G_3 represent possible realizations of the reliability of the three grids.

Arcs $\mathcal{A} = \{(i, j), i, j \in N\}$ represent the dependencies between chance nodes, decision nodes, and the value node. The *information (parent) set* $I(j)$ of a node j contains the chance or decision nodes from which there is a direct arc to it (i.e.; $I(j) = \{i \in C \cup D \mid (i, j) \in \mathcal{A}\}$). The Cartesian product of the possible states of the nodes in the parent set of j is denoted by $S_{I(j)}$. Thus, for each $i \in I(j)$, the *information state* $s_{I(j)} \in S_{I(j)}$ specifies the corresponding state of node i.

For a chance node $j \in C$, the state s_j is a realization of the random variable X_j. For a decision node $j \in D$, X_j is a decision variable whose state s_j indicates the decision taken at that node. Technically, the decisions are represented by binary variables $z(s_j) = 1$ if and only if $X_j = s_j$.

The state of a chance node $j \in C$ depends on the states of the nodes in its parent set, so that the probability of state s_j at chance node $j \in C$ is conditioned on the states of the nodes in its parent set

$$\mathbb{P}(X_j = s_j \mid X_{I(j)} = s_{I(j)}), \tag{9}$$

where $X_{I(j)} = s_{I(j)}$ means that variables $X_i, i \in I(j)$ take the corresponding value $s_i, i \in I(j)$.

A *path* in the influence diagram corresponds to a sequence $s = (s_j)_{j \in C \cup D}$ which contains one state for each chance and decision node. In particular, a path specifies a combination of realizations for hazards, global and local reinforcement actions, and the ensuing reliability of the grids associated with hazards and actions. Therefore, each path s has an associated disutility $\mathcal{U}(s)$ as stated in (4). Because the states of chance nodes are governed by probability distributions, these distributions, together with the decisions taken at decision nodes, imply that the paths occur with some probabilities. Specifically, the probability of path s is denoted by $\pi(s)$.

The expected disutility, expressed in (5), can now be expressed as $\sum_s \pi(s)\, \mathcal{U}(s)$ where the summation is taken over all paths. An upper bound of the probability of path $\pi(s)$ is given by accounting only for the chance nodes in the path

$$p(s) = \prod_{j \in C} \mathbb{P}(X_j = s_j \mid X_{I(j)} = s_{I(j)}). \tag{10}$$

The portfolio of reinforcement actions that minimizes the expected disutility of the DSO can now be determined by solving the MILP (11)-(15). Constraints (12) ensure that only one decision is made at each decision node, for example, at D_G, one can choose the state $s_j = (MC_0, ST_1)$ or $s_j = (MC_1, ST_1)$ but not both. Constraints (13) impose upper bounds on path probabilities. Constraints (14) enforce that the path probabilities can be positive only if the decisions along this path are taken. Constraints (15) define the binary decision variables.

$$\min_{z} \quad \sum_{s} \pi(s)\, \mathcal{U}(s) \tag{11}$$

$$\text{s.t.} \quad \sum_{s_j \in S_j} z(s_j) = 1, \qquad \forall j \in D \tag{12}$$

$$0 \le \pi(s) \le p(s), \qquad \forall s \tag{13}$$

$$\pi(s) \le z(s_j), \qquad \forall s,\ j \in D \tag{14}$$

$$z(s_j) \in \{0, 1\}, \qquad \forall j \in D,\ s_j \in S_j \tag{15}$$

3.5. Numerical results: complete information

We first present results under the assumption of complete information about the scenario probabilities and the DSO's priorities for reliability indices and grids. The grids are taken to be of equal importance, using uniform grid weights $w = (\frac{1}{3}, \frac{1}{3}, \frac{1}{3})$. The scenario probabilities are the estimations of Expert 1 in Table 9. The optimal portfolios are computed at different investment levels for each of the preferences about the reliability indices in Table 6.

3.5.1. Optimal portfolios

The optimal portfolios for each case and the varying total investment levels are in Figure 3. These portfolios minimize the aggregate expected disutility for a given investment level and reliability index case. The optimal portfolios are unequivocal, given that the information about DSO's priorities is completely specified. For example, if the investment level is 800, and the DSO is focused on improving the SAIDI reliability index (Case 1), the DSO should choose the portfolio[5] a_{59247} which consists of both global actions: spare transformer and maintenance crew, CS_+ and UL_{++} for Grid 2 and CS_{++}, UL_+ for Grid 3. On the other hand, if the DSO seeks to improve SAIFI (Case 2), the recommended portfolio is a_{15129}. In general, the distribution of the points in Figure 3 allows the DSO to make informed decisions about the investment level in recognition of the corresponding reliability impacts. In particular, this figure shows how increasing the investment level offers diminishing marginal improvements in reliability because the most impactful reinforcement actions are implemented first. This is common in reliable systems in which additional reinforcement actions tend to contribute less to improving reliability than those in unreliable systems.

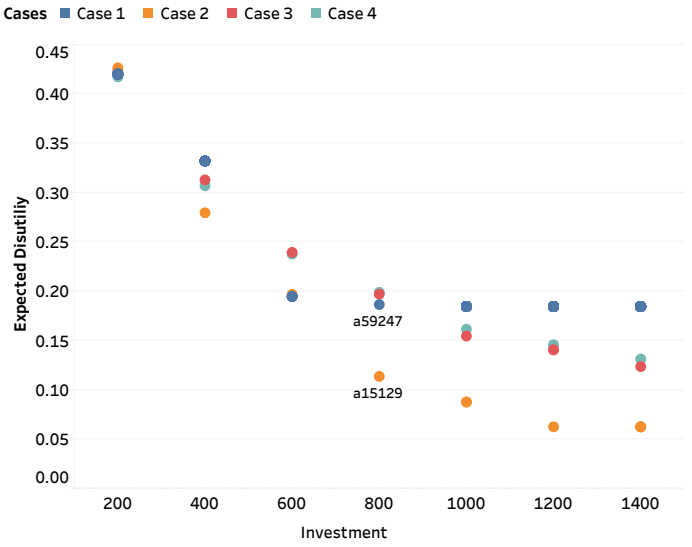

Figure 3: Optimal portfolios for different investment levels and priorities for reliability indices (Cases), based on the scenario probabilities of Expert 1.

[5]The composition of the portfolios in terms of the global actions and local actions for each grid can be found in [69]

3.5.2. Probability distribution over aggregate disutilities

Because the reliability of the grids depends on the scenarios, the aggregate disutility realized for the DSO is uncertain. It is, therefore, instructive to examine the cumulative distribution functions (CDF) to assess the probabilities with which the realized aggregate disutility will be below any given level. We denote by $F_{U_{tot}}$ the cumulative distribution function of the aggregate disutility. Thus, the CDF $F_{U_{tot}}(\bar{U}) = \mathbb{P}[U_{tot} \leq \bar{U}]$ gives the probability of having a disutility lower than or equal to the disutility level $\bar{U}$.

The CDFs of aggregate disutilities (4) are shown on the left and right sides of Figure 4 for Case 1 (focus on SAIDI) and Case 2 (focus on SAIFI), respectively. Generally, CDFs associated with higher investment levels are above those for lower levels because increased investments decrease the probability of higher disutilities. CDFs are more sensitive to the investment level for the SAIFI reliability index, suggesting that increasing investment will have a more significant impact on reducing aggregate disutility when measured by this index. On the other hand, if SAIDI is the only index, the CDFs are less sensitive to investment level, and increments beyond 500 do not reduce the aggregate DSO disutility in the first $\approx 60\%$ of the scenarios. Still, it reduces it for $\approx 40\%$ of the worst cases.

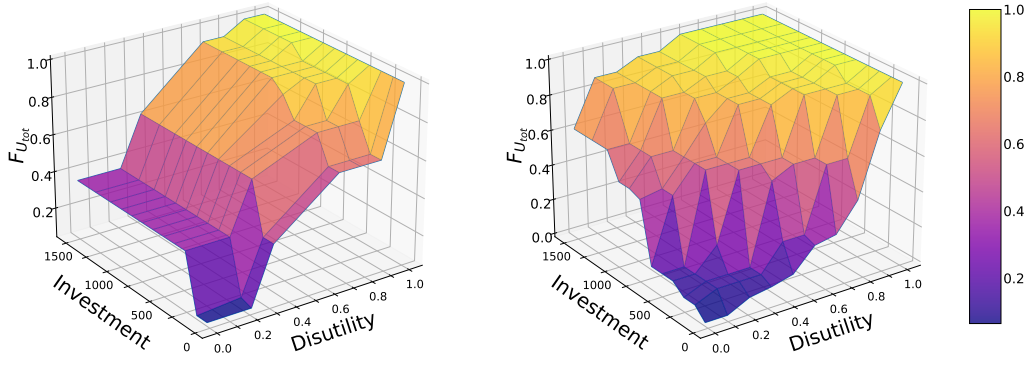

Figure 4: Cumulative distribution function of the disutility for Case 1 (SAIDI, left) and Case 2 (SAIFI, right). Probabilities correspond to the estimate of Expert 1.

3.6. Numerical results: partial information

We analyze partial information by examining non-dominated portfolios for four increasingly informative information sets representing the specification of scenario probabilities and the DSO's priorities for reliability indices and the grids. The first information set 1 (IS1) contains no preferences over the grids and thus allows for the possibility that

the focus is on any one of the three grids; the combination of the five experts represents the scenario probabilities and priorities for the reliability indices, including all combinations of the four cases listed in Table 6. The second information set 2 (IS2) is the same as IS1 regarding grid weights and scenario probabilities, but priorities for the reliability indices are narrowed down to Case 4. The third information set 3 (IS3) is the same as IS1, except that equal weights are assigned to the distribution grids. Note that IS3 is not contained in IS2 because it makes less restrictive assumptions about the priorities for reliability indices. The fourth information set 4 (IS4) contains complete information, considering the probabilities of Expert 1, the grids equally important, and the preferences over reliability indices of Case 4.

3.6.1. Non-dominated portfolios

Table 12 lists the number of non-dominated portfolios for the above information sets and alternative investment levels. The number of feasible portfolios depends on the investment level, which also affects the number of non-dominated portfolios. At a very low investment level, only a few reinforcement actions can be afforded; hence, there are relatively few non-dominated portfolios. When the available investment increases above 700, the number of non-dominated portfolios becomes smaller. This is because it is possible to implement relatively costly portfolios of reinforcement actions that outperform other portfolios. Also, because a reinforcement action cannot degrade the performance of the grids in any scenario, it is always better to implement an action than not to do so. Thus, if feasible, a portfolio that includes all possible reinforcement actions will perform at least as well as any other one that does not include all these actions.

Overall, incorporating additional information reduces the number of non-dominated portfolios. The information set IS1 is the least informative and leads to more non-dominated portfolios at all investment levels. Moreover, any non-dominated portfolio for the other information sets is also non-dominated for IS1. Incorporating information about priorities for the distribution grids (IS3) reduces the number of non-dominated portfolios more than incorporating information about priorities for the reliability indices (IS2). The DSO can use this result to identify which uncertainty is worth reducing to guide further elicitation toward achieving more conclusive results. For example, if the non-dominated portfolios are not that sensitive to the preferences regarding reliability indices but change depending on the scenario probabilities, focusing the effort on refining these probabilities would be recommended. On the other hand, eliciting priorities between reliability indices would not be necessary.

3.6.2. Core indices for reinforcement actions

The core index values for the global reinforcement actions in Figure 5 help the DSO choose reinforcement actions based on partial information. For example, if the priorities for the reliability indices are fully specified (IS2), the maintenance crew should be selected if the investment level is 1000 or higher. Moreover, the core index values also

Table 12
Number of non-dominated portfolios for different investment levels and information sets.

Investment level	IS1	IS2	IS3	IS4
400	264	83	26	1
700	432	140	20	1
1000	114	57	22	1
1300	6	5	2	1
1600	2	2	2	2

help discard some actions. For example, in IS2, the spare transformer has a core index of zero at investment level 400. Therefore, the spare transformer should be discarded if the DSO cannot increase the investment level beyond this. The same recommendation applies to information sets IS3 and IS4.

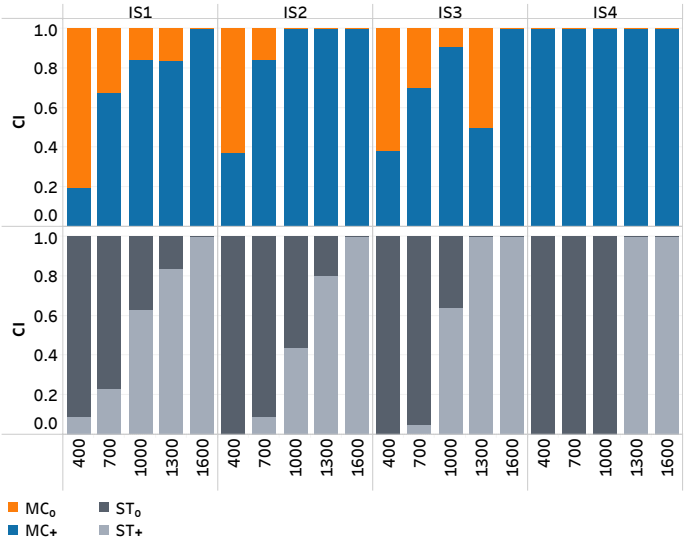

Figure 5: Core index of the global reinforcement actions for different information sets and investment levels.

The core index values for the local underground lines in Grid 1 are in Figure 6. Using the grid priorities of the information set IS3 increases the core index of UL_{++}. If the investment level exceeds 1300, the index becomes one, so UL_{++} is a clear recommendation. On the other hand, UL_{+} can be discarded for investment levels below 700. In some cases, providing more information can improve the relative standing of reinforcement actions with a small core index. For example, for an investment level of 1000, the action UL_0 has a core index of 0.25 in IS1. However, if the model parameters are fully specified, as in IS4, this action becomes part of the optimal portfolio. Thus, actions with a small but positive core index should not be discarded without a more detailed assessment of their contribution.

The core indices for the local reinforcement actions on Grid 3 are in Figure 7. Obtaining more information about grid priorities (S1 to S3) impacts recommendations concerning communication system updates and underground lines. Nevertheless, it has no impact on the recommendations regarding installing protective devices. Moreover, installing

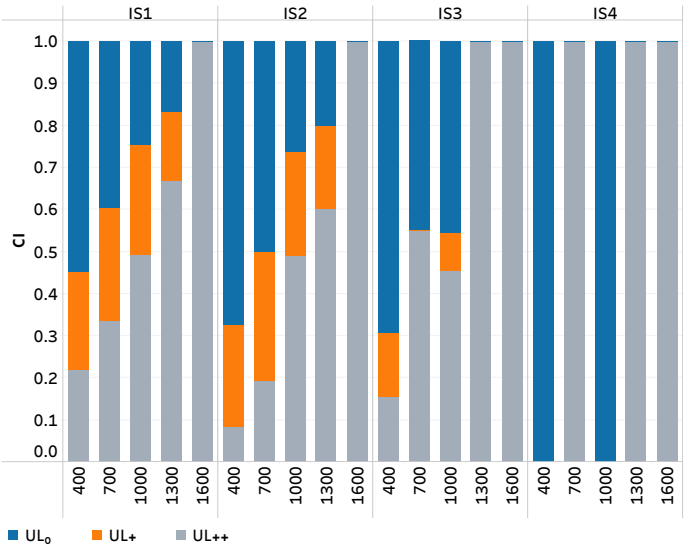

Figure 6: Core index values for local reinforcement actions associated with underground lines on Grid 1 for different information sets and investment levels.

protective devices on three lines of Grid 3 (PR_+) can be discarded because its core index is zero, meaning that this reinforcement action does not appear in any non-dominated portfolio.

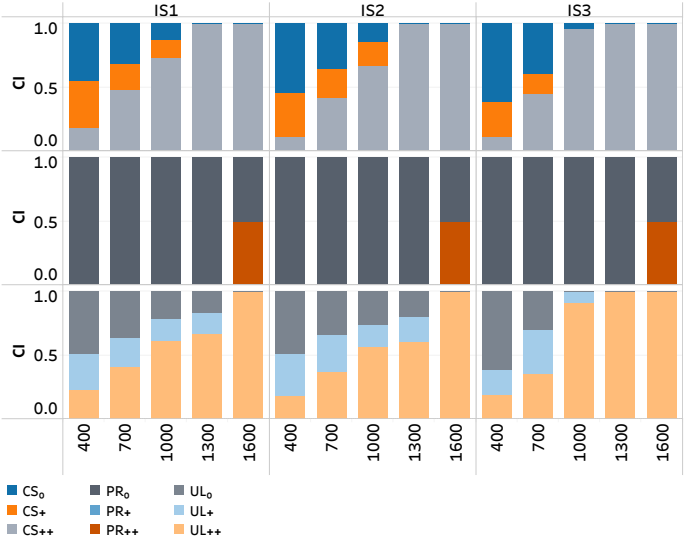

Figure 7: Core index of the local reinforcement actions on Grid 3 for different information sets and investment levels.

3.7. Decision recommendations

A challenge in analyzing non-dominated portfolios is that many of these can exist. For example, at the investment level 1000, there are 114 non-dominated portfolios for the information set IS1. Here, examination of core index values helps identify actions that should or should not be selected. Together, the non-dominated portfolios and core indices

narrow down the set of alternatives. Overall, the incorporation of partial information serves to focus attention on those reinforcement actions that are viable in view of such information; but because several non-dominated portfolios may remain, the question as to what principles should be adopted to make choices among these needs to be addressed.

Decision rules (see, e.g., [71]) can be relied on to guide selections among non-dominated portfolios, especially if partial information cannot be more precisely specified. The choice of the appropriate rule may need to be derived from broader concerns in justifying the decision. For example, to embrace the notion of conservatism, one may choose the minimax rule, which, in the present model, recommends the portfolio for which the maximum expected disutility for all possible parameters in the feasible information sets is the lowest. This is formulated as

$$Pmax = \arg\min_{a \in A} \max_{(p,w,\omega) \in S} U_{tot}. \tag{16}$$

To illustrate the use of the minimax rule, the disutilities for four of the 114 non-dominated portfolios for information set IS1 at the investment level of 1000 are in Figure 8. Each point represents the expected disutility for different parameters (p, w, ω) in IS1. Some choices of the parameters (p, w, ω) are indicated in color to emphasize that none of these portfolios dominate the other three. Nevertheless, the second portfolio has the minimum maximum disutility, so according to the minimax rule, it should be selected out of these four.

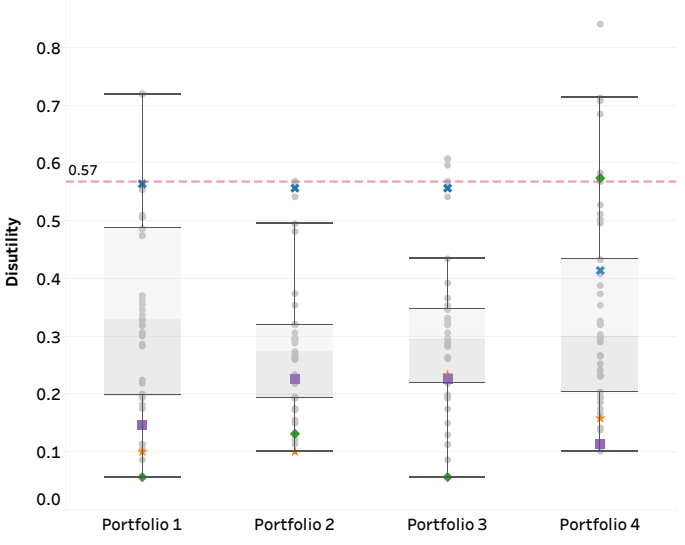

Figure 8: Disutilities for four 4 of the 114 non-dominated portfolios for a selection of parameters (p, w, ω) in the information set IS1. The red line marks the minimum maximum disutility.

3.8. Implementation details and computational feasibility

The optimization model for complete information was implemented using Gurobi 9.5.2 as the solver, Julia 1.7.3 as the programming language, and JuMP 1.17 combined with the DecisionProgramming 1.2 package for the

MILP formulation. The Algorithms in Appendix A to obtain non-dominated portfolios for partial information were implemented in Python 3.10.5 for data management using the same Gurobi, Julia, and JuMP versions to run the optimization model. Because Algorithm 2 can be parallelized, the computational bottleneck is the optimization model. To assess its computational performance, we sampled 30 random scenario probability sets and solved the MILP model for different investment levels, considering the three grids equally important and the importance of reliability indices according to Case 1. Table 13 shows the computation times for a standard laptop with an Intel Core i5-1135G7 processor (2.4 GHz) and 16 GB of RAM. The computation times are relatively low (under three minutes), recognizing that the framework is intended for planning purposes, where there is more time for optimization than in real-time operational contexts.

Table 13
Summary statistics of computational time (in seconds) for different budget levels.

Budget	150	250	400	600	900	1300
Average (s)	3.5	11.8	32.1	91.3	91.7	50.4
Min (s)	3.3	10.8	24.0	76.6	61.0	44.5
Max (s)	4.4	14.8	46.9	124.0	130.5	68.4

The number of feasible reinforcement portfolios tends to grow with more alternative reinforcement actions. However, the number of such actions is usually limited. This is because (i) DSOs generally adhere to standardized reinforcement procedures; (ii) the parameters associated with the impact of reinforcement actions on failure rates or restoration times must be estimated. This can be done using models like those described at the end of Section 2.5.2 or through expert elicitation. The number of reinforcement actions that can be meaningfully considered is limited by the confidence about the estimated parameters and the availability of models or experts to provide them; (iii) the cost of the reinforcement actions needs to be determined, which in some cases requires further studies. For example, the construction cost of underground lines depends on many factors such as the type of soil, the price of the land, the length of the line, etc. In our case study, we have 78,000 feasible portfolios, which suggests that the framework can handle sizable yet realistic problems with acceptable computation times. Additionally, the computation of portfolios for different budgets and the sensitivity analyses of model parameters can be conducted in parallel. The framework is not limited to the solver or the strategy to solve the influence diagrams. In this regard, promising computational improvements have been made by converting influence diagrams into rooted junction trees [72]. For example, partial support for rooted junction trees has already been implemented in DecisionProgramming 2.0 [70].

4. Discussion

Our numerical results illustrate the benefits of systematically evaluating portfolios of reinforcement actions within a structured framework. As the size of the problem increases (e.g., more hazards, grids, or reinforcing actions),

there will be computational challenges that call for an appropriate level of granularity in modeling hazards and conditional reliabilities. Even so, the computation of non-dominated portfolios for relatively streamlined models can be helpful because this can be done relatively easily, and subsequent sensitivity analyses can be carried out to assess the recommended portfolios. From this perspective, the framework can be viewed as an approach that admits partial information in the screening of viable portfolios of reinforcement actions, which can then be subjected to closer scrutiny.

Because the values of numerical parameters, including scenario probabilities, priority weights, and impact factors, may be uncertain, it is instructive to conduct sensitivity analyses to explore how the recommendations would change if the parameters are perturbed from their baseline levels. Such analyses may also help direct efforts toward improving the accuracy of these parameters. They may also help identify joint ranges of parameter values within which the recommended portfolios remain optimal or determine threshold levels where one portfolio could be replaced by another.

An assumption in the development of this framework is that the reinforcement actions remain effective for the same length of time (i.e., planning period) and that the resources they require are also attributed to such a single period. If this is not the case, one can still use the one-period model as an approximation by considering (i) how long the actions will remain effective and (ii) how much of their costs can be meaningfully attributed to a single period [73]. Alternatively, it would be possible to convert the current single-period model into a multi-period one, which would be much larger. Such dynamic models would be warranted if the hazards are not static. For example, this would be the case with variable weather conditions during winter and summer.

The current framework assumes that the reliability of one grid does not affect the reliability of the others. This assumption can be relaxed to examine interconnected systems in which a disruption in one grid can lead to cascading effects, such as overloading neighboring grids. Such interdependencies are relevant when analyzing not only power grids but also other critical infrastructures, such as water supply, transportation, or gas networks, where failures in one system can propagate to others. From a modeling perspective, the influence diagram presented in Section 2.4.1 can be extended by introducing additional arcs between the chance nodes that represent the reliability of interconnected networks. From a data perspective, this extension would also require sufficient coordination and information sharing among the infrastructure managers in charge of these networks to quantify relevant interdependencies and provide a stronger basis for improving overall system reliability.

Another extension is to incorporate reinforcement actions that affect scenario probabilities: in this case, the hazards will no longer be exogenous but, rather, endogenous uncertainties as the reinforcement actions can shape the information set of corresponding scenario probabilities. Methodologically, the influence diagram in Figure 1 would, in

this case, need to be expanded by another layer containing the initial and revised hazards separately. Such an extension will lead to a substantially larger model, which could be built along the lines considered by [74].

5. Conclusion

The proposed framework helps DSOs make well-founded selections among reinforcement actions to build portfolios that offer the desired balance between investment levels and improvements in reliability. It delivers robust decision-making recommendations based on the assessment of individual reinforcement actions and the analysis of investment portfolios, recognizing that partial (rather than complete) information may be available from sources such as reliability models, DSO preferences, and expert judgments. One of the benefits of the framework is that it supports iterative decision processes that offer preliminary results early on to guide the elicitation of further information as a step toward more conclusive results. Although computational challenges can be encountered, sensitivity analyses and suggested model extensions can be used to adapt the framework to a broad range of contexts. Expanding its scope to account for interdependencies between networks and endogenous uncertainties, for example, can further enhance its relevance to complex, interconnected systems.

CRediT authorship contribution statement

Joaquín de la Barra: Conceptualization of this study, Methodology, Software, Data curation, Writing - Original draft preparation. **Ahti Salo:** Conceptualization of this study, Methodology, Writing - Original draft. **Mahdi Pourakbari-Kasmaei:** Conceptualization of this study, Methodology, Writing - Original draft.

A. Identification of dominance and computation of non-dominated portfolios

Algorithm 1 determines if portfolio a dominates portfolio a' for the given information set S. For a formal proof of the dominance condition, see Theorem 1 in [66]. In **Step 1**, the extreme points of the information set S are identified. In **Step 2**, the maximum difference in disutility between the two portfolios across the information set is computed. In **Step 3**, the minimum difference in disutility is calculated. In **Step 4**, the maximum and minimum differences of the disutilities are compared to determine whether one portfolio dominates the other. The algorithm returns "True" (**Step 5**) if a dominates a', and "False" otherwise (**Step 7**).

Algorithm 2 computes the non-dominated portfolios for a given information set S. In **Step 1**, the extreme points of the information set S are identified. In our case study, these points are input parameters of the model such that the information set S consists of these points and their linear combinations. If the information set is defined by linear inequality constraints on the parameters, the corresponding extreme points can be efficiently computed using linear programming techniques [see, e.g., 75]

Algorithm 1 Check if portfolio a dominates a' in the information set S

$S^* \leftarrow$ The set of extreme points of the information set S
$\Delta_{\max} \leftarrow \max_{(p,w,\omega)\in S^*} \left\{\mathbb{E}[U_{tot}(p,w,\omega,h,a)] - \mathbb{E}[U_{tot}(p,w,\omega,h,a')]\right\}$
$\Delta_{\min} \leftarrow \min_{(p,w,\omega)\in S^*} \left\{\mathbb{E}[U_{tot}(p,w,\omega,h,a)] - \mathbb{E}[U_{tot}(p,w,\omega,h,a')]\right\}$
if $\Delta_{\max} \leq 0$ **and** $\Delta_{\min} < 0$ **then**
    return True
else
    return False
end if

In **Step 2**, the optimal portfolio of reinforcement actions for each extreme point is determined by solving the MILP optimization model that corresponds to the influence diagram in Figure 1. These portfolios are, by definition, non-dominated, as they minimize disutility at some extreme point of the information set. In **Step 3**, the initial set of non-dominated portfolios is formed from these optimal solutions. **Steps 4–10** iterate over all the portfolios that are feasible in that they satisfy budget and logical constraints. In **Step 5**, each new candidate portfolio a is compared to the previously computed set of non-dominated portfolios using Algorithm 1. If the new portfolio a is non-dominated, it is added to the set in **Step 6**. Moreover, the set of non-dominated portfolios is updated, removing all portfolios dominated by a in **Step 7**. Otherwise, a is dominated and, therefore, is discarded in Step 9. Finally, the algorithm returns all non-dominated portfolios in **Step 12**.

Algorithm 2 Compute $\mathcal{A}_N(S)$

$S^* \leftarrow$ The set of extreme points of the information set S
$\mathcal{A}^*(S) \leftarrow$ The set containing the optimal portfolio at each extreme point
$\mathcal{A}_N(S) \leftarrow \mathcal{A}^*(S)$ Initialize the set of non-dominated portfolios
for $a \in \mathcal{A}_F$ **do**
    if Algorithm 1(a', a) = **False** $\quad \forall a' \in A_F$ **then**
        $\mathcal{A}_N(S) \leftarrow \mathcal{A}_N(S) \cup a$
        $\mathcal{A}_N(S) \leftarrow \mathcal{A}_N(S) \setminus \left\{a' \in \mathcal{A}_N(S) \setminus \mathcal{A}^*(S) \mid \text{Algorithm 1}(a, a') = \textbf{True}\right\}$
    else
        Discard portfolio a
    end if
end for
return $\mathcal{A}_N(S)$

Algorithm 2 can be parallelized to improve computational efficiency. First, the optimal portfolios at each extreme point can be computed independently. Second, the set of feasible portfolios can be partitioned into subsets so that the corresponding non-dominated portfolios are first determined within each subset, whereafter the final set of all non-dominated portfolios is computed by carrying out pairwise dominance checks across these subsets.

References

[1] F. Wirtz, Influence on reliability of supply and its marginal costs in medium-voltage networks, in: 2007 IEEE Lausanne Power Tech, 2007, pp. 1623–1628. doi:10.1109/PCT.2007.4538558.

[2] J. Wu, L. Zhang, Y. Bai, G. Reniers, A safety investment optimization model for power grid enterprises based on system dynamics and bayesian network theory, Reliability Engineering & System Safety 221 (2022) 108331.

[3] P. S. Kundur, O. P. Malik, Power System Stability and Control, McGraw-Hill Education, 2022.

[4] R. Billinton, R. Allan, Power-system reliability in perspective, Electronics and Power 30 (1984) 231–236.

[5] C. Ji, Y. Wei, H. Mei, J. Calzada, M. Carey, S. Church, T. Hayes, B. Nugent, G. Stella, M. Wallace, J. White, R. Wilcox, Large-scale data analysis of power grid resilience across multiple us service regions, Nature Energy 1 (2016) 16–52.

[6] L. Shang, R. Hu, T. Wei, H. Ci, W. Zhang, H. Chen, Multiobjective optimization for hybrid AC/DC distribution network structure considering reliability, in: 2021 IEEE Sustainable Power and Energy Conference (iSPEC), 2021, pp. 3034–3041. doi:10.1109/iSPEC53008.2021.9735745.

[7] L. Zhang, W. Tang, Y. Liu, T. Lv, Multiobjective optimization and decision-making for DG planning considering benefits between distribution company and DGs owner, International Journal of Electrical Power & Energy Systems 73 (2015) 465–474.

[8] X.-R. Lei, Z. Ren, W.-Y. Huang, B.-Y. Chen, Fuzzy reliability analysis of distribution systems accounting for parameters uncertainty, in: 2005 International Conference on Machine Learning and Cybernetics, volume 7, 2005, pp. 4017–4022. doi:10.1109/ICMLC.2005.1527640.

[9] P. Shi, Y. Li, Y. Du, Q. Cai, H. Chen, Distribution network planning considering uncertainty of incremental distribution network access, in: 2020 IEEE 4th Conference on Energy Internet and Energy System Integration (EI2), 2020, pp. 2244–2247. doi:10.1109/EI250167.2020.9347026.

[10] M. A. Mahmoud, N. R. Md Nasir, M. Gurunathan, P. Raj, S. A. Mostafa, The current state of the art in research on predictive maintenance in smart grid distribution network: Fault's types, causes, and prediction methods—A systematic review, Energies 14 (2021).

[11] E. Tosoni, A. Salo, J. Govaerts, E. Zio, Comprehensiveness of scenarios in the safety assessment of nuclear waste repositories, Reliability Engineering & System Safety 188 (2019) 561–573.

[12] A. Salo, E. Tosoni, J. Roponen, D. W. Bunn, Using cross-impact analysis for probabilistic risk assessment, Futures & Foresight Science 4 (2022) e2103.

[13] I. Šarūnienė, L. Martišauskas, R. Krikštolaitis, J. Augutis, R. Setola, Risk assessment of critical infrastructures: A methodology based on criticality of infrastructure elements, Reliability Engineering & System Safety 243 (2024) 109797.

[14] R. Bradfield, G. Wright, G. Burt, G. Cairns, K. Van Der Heijden, The origins and evolution of scenario techniques in long range business planning, Futures 37 (2005) 795–812.

[15] H. Carlsen, E. Eriksson, K. Dreborg, B. Johansson, O. Bodin, Systematic exploration of scenario spaces, Foresight 18 (2016) 59–75.

[16] G. Hou, K. K. Muraleetharan, V. Panchalogaranjan, P. Moses, A. Javid, H. Al-Dakheeli, R. Bulut, R. Campos, P. S. Harvey, G. Miller, K. Boldes, M. Narayanan, Resilience assessment and enhancement evaluation of power distribution systems subjected to ice storms, Reliability Engineering & System Safety 230 (2023) 108964.

[17] J. Jasiūnas, T. Heikkinen, P. D. Lund, I. Láng-Ritter, Resilience of electric grid to extreme wind: Considering local details at national scale, Reliability Engineering & System Safety 232 (2023) 109070.

[18] M. Atrigna, A. Buonanno, R. Carli, G. Cavoney, P. Scarabaggioy, M. Valenti, G. Graditi, M. Dotoli, Effects of heatwaves on the failure of power distribution grids: a fault prediction system based on machine learning, in: 2021 IEEE International Conference on Environment and Electrical Engineering and 2021 IEEE Industrial and Commercial Power Systems Europe (EEEIC / I&CPS Europe), 2021, pp. 1–5.

doi:10.1109/EEEIC/ICPSEurope51590.2021.9584751.

[19] X. Diao, Y. Zhao, C. Smidts, P. K. Vaddi, R. Li, H. Lei, Y. Chakhchoukh, B. Johnson, K. L. Blanc, Dynamic probabilistic risk assessment for electric grid cybersecurity, Reliability Engineering & System Safety 241 (2024) 109699.

[20] J. Ding, A. Qammar, Z. Zhang, A. Karim, H. Ning, Cyber threats to smart grids: Review, taxonomy, potential solutions, and future directions, Energies 15 (2022).

[21] A. Bagheri, H. Monsef, H. Lesani, Integrated distribution network expansion planning incorporating distributed generation considering uncertainties, reliability, and operational conditions, International Journal of Electrical Power & Energy Systems 73 (2015) 56–70.

[22] Y. Fan, X. Jing, Z. Zhang, L. Yingying, L. Shuyong, An overview of research on affecting factors of distribution network reliability, in: 2016 China International Conference on Electricity Distribution (CICED), 2016, pp. 1–4. doi:10.1109/CICED.2016.7576097.

[23] J. Pan, X. Hou, B. Xu, L. Kou, Weaknesses identification using reliability tracking in distribution system with distribution generation, in: 2019 IEEE Innovative Smart Grid Technologies - Asia (ISGT Asia), 2019, pp. 3407–3412. doi:10.1109/ISGT-Asia.2019.8881645.

[24] L. C. Dias, A. Morton, J. Quigley, Elicitation: State of the Art and Science, Springer International Publishing, Cham, 2018, pp. 1–14. doi:10.1007/978-3-319-65052-4_1.

[25] Finnish Ministry of the Interior, National risk assessment 2018, Publications of the Ministry of the Interior 73 (2019) 1–69.

[26] N. Amjady, A. Attarha, S. Dehghan, A. J. Conejo, Adaptive robust expansion planning for a distribution network with DERs, IEEE Transactions on Power Systems 33 (2018) 1698–1715.

[27] G. Muñoz-Delgado, J. Contreras, J. M. Arroyo, Distribution network expansion planning with an explicit formulation for reliability assessment, IEEE Transactions on Power Systems 33 (2018) 2583–2596.

[28] S.-A. Ahmadi, V. Vahidinasab, M. S. Ghazizadeh, K. Mehran, D. Giaouris, P. Taylor, Co-optimising distribution network adequacy and security by simultaneous utilisation of network reconfiguration and distributed energy resources, IET Generation, Transmission & Distribution 13 (2019) 4747–4755.

[29] A. Azizivahed, A. Arefi, S. Ghavidel, M. Shafie-khah, L. Li, J. Zhang, J. P. S. Catalão, Energy management strategy in dynamic distribution network reconfiguration considering renewable energy resources and storage, IEEE Transactions on Sustainable Energy 11 (2020) 662–673.

[30] M. Tian, Z. Zhu, Z. Dong, L. Zhao, H. Yao, Resilience enhancement of cyber–physical distribution systems via mobile power sources and unmanned aerial vehicles, Reliability Engineering & System Safety 254 (2025) 110603.

[31] B. Sambasivam, C. Colombe, J. J. Hasenbein, B. D. Leibowicz, Optimal resource placement for electric grid resilience via network topology, Reliability Engineering & System Safety 245 (2024) 110010.

[32] T. Zhao, H. Tu, R. Jin, Y. Xia, F. Wang, Improving resilience of cyber–physical power systems against cyber attacks through strategic energy storage deployment, Reliability Engineering & System Safety 252 (2024) 110438.

[33] H. Hou, W. Wu, Z. Zhang, R. Wei, L. Wang, H. He, Z. Y. Dong, A tri-level typhoon-dad robust optimization framework to enhance distribution network resilience, Reliability Engineering & System Safety 245 (2024) 110004.

[34] J. de la Barra, A. Angulo, E. Gil, A model for simultaneous location and coordination of protective devices in radial distribution networks, IET Generation, Transmission & Distribution 15 (2021) 2734–2746.

[35] J. Franco, M. J. Rider, J. López, Optimization-based switch allocation to improve energy losses and service restoration in radial electrical distribution systems, IET Generation Transmission & Distribution 10 (2016) 2792–2801.

[36] J. Kennedy, P. Ciufo, A. Agalgaonkar, A review of protection systems for distribution networks embedded with renewable generation, Renewable and Sustainable Energy Reviews 58 (2016) 1308–1317.

[37] A. H. Osman, M. S. Hassan, M. Sulaiman, Communication-based adaptive protection for distribution systems penetrated with distributed generators, Electric Power Components and Systems 43 (2015) 556–565.

[38] S. Ganguly, N. C. Sahoo, D. Das, Recent advances on power distribution system planning: A state-of-the-art survey, Energy Systems 4 (2013) 165–193.

[39] S. Gururajapathy, H. Mokhlis, H. Illias, Fault location and detection techniques in power distribution systems with distributed generation: A review, Renewable and Sustainable Energy Reviews 74 (2017) 949–958.

[40] A. Salo, J. Keisler, A. Morton, An Invitation to Portfolio Decision Analysis, Springer New York, New York, NY, 2011, pp. 3–27. URL: https://doi.org/10.1007/978-1-4419-9943-6_1. doi:10.1007/978-1-4419-9943-6_1.

[41] A. Salo, J. Andelmin, F. Oliveira, Decision programming for mixed-integer multi-stage optimization under uncertainty, European Journal of Operational Research 299 (2022) 550–565.

[42] IEEE, IEEE Guide for Electric Power Distribution Reliability Indices, IEEE Std 1366-2012 (Revision of IEEE Std 1366-2003) (2012) 1–43.

[43] C. Werner, T. Bedford, R. M. Cooke, A. M. Hanea, O. Morales-Nápoles, Expert judgement for dependence in probabilistic modelling: A systematic literature review and future research directions, European Journal of Operational Research 258 (2017) 801–819.

[44] M. Lawrence, P. Goodwin, M. O'Connor, D. Önkal, Judgmental forecasting: A review of progress over the last 25years, International Journal of Forecasting 22 (2006) 493–518. Twenty five years of forecasting.

[45] J. Liesiö, A. Salo, Scenario-based portfolio selection of investment projects with incomplete probability and utility information, European Journal of Operational Research 217 (2012) 162–172.

[46] J. Roponen, A. Salo, A probabilistic cross-impact methodology for explorative scenario analysis, Futures & Foresigh Science (2023) e165.

[47] G. Muñoz-Delgado, J. Contreras, J. M. Arroyo, Reliability assessment for distribution optimization models: A non-simulation-based linear programming approach, IEEE Transactions on Smart Grid 9 (2018) 3048–3059.

[48] C. Reiz, T. Dias de Lima, J. Leite, M. Javadi, C. Gouveia, A multi-objective approach for the optimal placement of protection and control devices in distribution networks with microgrids, IEEE Access (2022) 1–13.

[49] Y. Wang, L. Chen, M. Yao, X. Li, Evaluating weather influences on transmission line failure rate based on scarce fault records via a bi-layer clustering technique, IET Generation, Transmission & Distribution 13 (2019) 5305–5312.

[50] J. Clavijo-Blanco, J. Rosendo-Macías, Failure rates in distribution networks: Estimation methodology and application, Electric Power Systems Research 185 (2020) 106398.

[51] K. Alvehag, L. Soder, A stochastic weather dependent reliability model for distribution systems, in: Proceedings of the 10th International Conference on Probablistic Methods Applied to Power Systems, 2008, pp. 1–8.

[52] Y. Zhou, A. Pahwa, S.-S. Yang, Modeling weather-related failures of overhead distribution lines, IEEE Transactions on Power Systems 21 (2006) 1683–1690.

[53] F. C. Macedo, F. Alminhana, L. F. Fadel Miguel, A. T. Beck, Performance-based reliability assessment of transmission lines under tornado actions, Reliability Engineering & System Safety 252 (2024) 110475.

[54] H. Liang, Q. Xie, Probabilistic seismic risk analysis of electrical substations considering equipment-to-equipment seismic failure correlations, Reliability Engineering & System Safety 253 (2025) 110588.

[55] A. Shafieezadeh, U. P. Onyewuchi, M. M. Begovic, R. DesRoches, Age-dependent fragility models of utility wood poles in power distribution networks against extreme wind hazards, IEEE Transactions on Power Delivery 29 (2014) 131–139.

[56] H. Ghasemi, E. Shahrabi Farahani, M. Fotuhi-Firuzabad, P. Dehghanian, A. Ghasemi, F. Wang, Equipment failure rate in electric power distribution networks: An overview of concepts, estimation, and modeling methods, Engineering Failure Analysis 145 (2023) 107034.

[57] S. A. Fenrick, L. Getachew, Cost and reliability comparisons of underground and overhead power lines, Utilities Policy 20 (2012) 31–37.

[58] W. Hughes, W. Zhang, D. Cerrai, A. Bagtzoglou, D. Wanik, E. Anagnostou, A hybrid physics-based and data-driven model for power distribution system infrastructure hardening and outage simulation, Reliability Engineering & System Safety 225 (2022) 108628.

[59] W. O. Taylor, P. L. Watson, D. Cerrai, E. N. Anagnostou, Dynamic modeling of the effects of vegetation management on weather-related power outages, Electric Power Systems Research 207 (2022) 107840.

[60] W. Hughes, P. L. Watson, D. Cerrai, X. Zhang, A. Bagtzoglou, W. Zhang, E. Anagnostou, Assessing grid hardening strategies to improve power system performance during storms using a hybrid mechanistic-machine learning outage prediction model, Reliability Engineering & System Safety 248 (2024) 110169.

[61] A. Mancuso, M. Compare, A. Salo, E. Zio, Optimal prognostics and health management-driven inspection and maintenance strategies for industrial systems, Reliability Engineering & System Safety 210 (2021) 107536.

[62] L. Neuvonen, M. Dillon, E. Vilkkumaa, A. Salo, M. Jäntti, S. Heinävaara, Optimizing the finnish colorectal cancer population screening program with decision programming, European Journal of Operational Research (2025).

[63] R. Billinton, R. Goel, An analytical approach to evaluate probability distributions associated with the reliability indices of electric distribution systems, IEEE Transactions on Power Delivery 1 (1986) 245–251.

[64] N. Balijepalli, S. Venkata, R. Christie, Modeling and analysis of distribution reliability indices, IEEE Transactions on Power Delivery 19 (2004) 1950–1955.

[65] A. Banerjee, S. Chattopadhyay, M. Gavrilas, G. Grigoras, Optimization and estimation of reliability indices and cost of Power Distribution System of an urban area by a noble fuzzy-hybrid algorithm, Applied Soft Computing 102 (2021) 107078.

[66] J. Liesiö, P. Mild, A. Salo, Preference programming for robust portfolio modeling and project selection, European Journal of Operational Research 181 (2007) 1488–1505.

[67] J. de la Barra Toloza, A. Salo, Selecting combinations of reinforcement actions to improve the reliability of distribution grids in the face of external hazards, in: Proceedings of the The 33rd European Safety and Reliability Conference (ESREL 2023), 3 – 8 September 2023, Southampton, UK, 2023, pp. 3320–3327. doi:10.3850/978-981-18-8071-1_P248-cd.

[68] J. Liesiö, P. Mild, A. Salo, Robust portfolio modeling with incomplete cost information and project interdependencies, European Journal of Operational Research 190 (2008) 679–695.

[69] J. de la Barra, Grids reliability data, 2023. URL: https://github.com/jdelab1/reinforcement_grids_data.

[70] F. Oliveira, O. Herrala, J. Tollander de Balsch, H. Hankimaa, J. Andelmin, T. Terho, E. Honkamaa, DecisionProgramming.jl, 2024. URL: https://github.com/gamma-opt/DecisionProgramming.jl. doi:10.5281/zenodo.13639605.

[71] E. Baker, V. Bosetti, A. Salo, Robust portfolio decision analysis: An application to the energy research and development portfolio problem, European Journal of Operational Research 284 (2020) 1107–1120.

[72] A. Parmentier, V. Cohen, V. Leclère, G. Obozinski, J. Salmon, Integer programming on the junction tree polytope for influence diagrams, INFORMS Journal on Optimization 2 (2020) 209–228.

[73] A. Mancuso, M. Compare, A. Salo, E. Zio, Portfolio optimization of safety measures for the prevention of time-dependent accident scenarios, Reliability Engineering & System Safety 190 (2019) 106500.

[74] E. Vilkkumaa, J. Liesiö, A. Salo, L. Ilmola-Sheppard, Scenario-based portfolio model for building robust and proactive strategies, European Journal of Operational Research 266 (2018) 205–220.

[75] H. Taha, Operations Research: An Introduction, Pearson Education, Inc, New Jersey, 2003.